

The influence of Greenland ice sheet melting on the Atlantic meridional overturning circulation during past and future warm periods: a model study

M. Blaschek · P. Bakker · H. Renssen

Received: 11 December 2013 / Accepted: 25 July 2014 / Published online: 6 August 2014
© Springer-Verlag Berlin Heidelberg 2014

Abstract The sensitivity of the climate system to changes in radiative forcing is crucial for our understanding of past and future climates. Especially important are feedbacks related to melting of ice sheets like the Greenland ice sheet (GIS) and its potential impact on the Atlantic meridional overturning circulation (AMOC). These effects are likely to delay and dampen predicted long-term warming trends. Estimates of climate sensitivity may be deduced from palaeoclimate-reconstructions, but this raises the question whether past climate sensitivity is applicable to the future. Therefore we have analysed the impact of GIS melt water on the AMOC strength in two past warm climates (last interglacial and early present interglacial) and three future scenarios with three different model parameter sets. These model parameter sets represent three different model sensitivities to freshwater perturbation: low, moderate and high. In both the moderate and high sensitivity versions, we find for lower GIS melt rates (below 54 mSv, $Sv = 10^6 \text{ m}^3/\text{s}$) a clear difference between past and future warm climates in the sensitivity of the AMOC to GIS melt. This difference is connected to the convective activity in the Labrador Sea and the amount of additional surface freshening due to sea ice melting. In contrast, for higher GIS melt rates (over 54 mSv) we find similar reductions of the AMOC strength in all cases. Considering the low sensitivity version of our model, we find that for all GIS melt rates the influence of freshwater forcing on the AMOC is independent of

the background climate. Our results and implications are thus strongly determined by the parameter set considered in our model. Nonetheless, our results from two out of three model versions suggest that proxy-based reconstructions of past AMOC sensitivity to GIS melt are likely to be misleading if interpreted for future applications.

Keywords Interglacials · Greenland ice sheet · Climate modelling · Climate sensitivity · AMOC · Sea ice

1 Introduction

It is fundamental to know the climate system response to changes in radiative forcing in order to understand future climate change. This response involves different feedbacks and recent studies (Roe 2009; Köhler et al. 2010; Lunt et al. 2010; Rohling et al., 2012; Zeebe 2013) emphasize the importance of so-called slow feedbacks, involving changes in ice sheets, vegetation, ocean circulation and biogeochemical cycles, to have a considerable effect on long-term climate sensitivity and result in a prolonged warming in simulations forced by future emission scenarios. One such feedback is related to the melting of the Greenland ice sheet (GIS) and its potential to weaken the Atlantic Ocean circulation strength. However, the impact of this slow feedback has until now hardly been taken into account in the IPCC AR4 ensemble projections of future climate change, with the exception of IPSLCM4 (Swingedouw et al. 2006, 2007; Schneider et al. 2007). Therefore, in this paper we study the impact of GIS melt on the behaviour of the Atlantic Meridional Overturning Circulation (AMOC) under warm past and future climate conditions.

The AMOC is part of the global ocean circulation and transports heat in the near-surface layer from the Tropics to

Electronic supplementary material The online version of this article (doi:10.1007/s00382-014-2279-1) contains supplementary material, which is available to authorized users.

M. Blaschek (✉) · P. Bakker · H. Renssen
Cluster Earth and Climate, Faculty of Earth and Life
Sciences, VU University Amsterdam, De Boelelaan 1085,
1081HV Amsterdam, The Netherlands
e-mail: m.blaschek@vu.nl

the Northern Hemisphere mid- and high-latitudes. Today the northward heat transport of 1.33 ± 0.4 PW at 26°N (Johns et al. 2011) in this current system contributes to a relatively warm Northern Hemisphere climate, in particular over Europe. This oceanic heat transport is dominated by the AMOC (88 % or 1.18 PW, Johns et al. 2011), that transforms northward moving relatively saline waters into North Atlantic Deep Water (NADW) and returns these waters southward in the deep ocean. Convection of waters from the surface to the deep ocean is largely determined by the heat exchange between ocean and atmosphere that is in turn sensitive to a stratification of the ocean surface and to the insulation effect of sea ice (Ganopolski and Rahmstorf 2001; Kuhlbrodt et al. 2007). In the North Atlantic basin there are at present three main regions where deep water formation occurs, in the Nordic Seas, Labrador Seas (e.g. Marshall and Schott 1999) and the Irminger Sea (Pickart et al. 2003).

Climate model simulations indicate that a projected temperature rise of up to 4.4 K by 2100 AD outlined by the IPCC AR4 (scenario A1B) is accompanied by more precipitation (globally 1 to 6 % more, Meehl et al. 2007) over the North Atlantic, higher river inflow as well as increased melt water discharge from the GIS (3–24 mSv until 2100 AD, Meehl et al. 2007). The expected increases in sea surface temperatures and precipitation over convection areas will lower sea surface density, and is expected to weaken deep convection, and thereby potentially decreasing the AMOC strength by 25 % at the end of this century (Schmittner et al. 2005; Meehl et al. 2007). The northward meridional heat transport is likely to follow this trend, unless it is compensated by a strengthened baroclinic gyre circulation as found by Drijfhout and Hazeleger (2006) in ensemble predictions of the near future. In simulations of the next century, the impact of enhanced melting of the GIS has mostly been neglected in IPCC AR4-type models (Meehl et al. 2007; Srokosz et al. 2012) as well as in the recent update AR5 (CMIP5, Weaver et al. 2012). There are a few exceptions, such as the studies by Fichefet (2003), Swingedouw et al. (2007) or Hu et al. (2011). The latter found that only high GIS melt rates (a total of ~ 0.3 Sv over 100 years) will cause a significant weakening of the AMOC and indicate that AMOC-induced cooling is not likely to overcome greenhouse-induced warming. This confirms a previous result from Ridley et al. (2005), who found a complete retreat of the GIS within 3,000 years, but only small long-term effects on the global climate employing a GCM coupled to a dynamical ice sheet model.

All climate model predictions crucially depend on the Earth system's sensitivity of the model under consideration. In climate models, Earth system's sensitivity is not a single tuneable parameter, but the net effect of all included processes and their parameterizations, as well as all internal feedbacks. The AMOC's sensitivity to GIS melt is one

part of the Earth system sensitivity and thus relevant for evaluation of future projections. However, large uncertainty remains concerning the AMOC's sensitivity (Stouffer et al. 2006), its stability (Hofmann et al. 2009) and its long-term impact on the Earth system's sensitivity (Meehl et al. 2007; Zeebe 2013). Studying the relation between the AMOC and GIS melt in the past can help constrain the impact of GIS melt on the climate sensitivity to freshwater perturbations. In a model study of past, present and future AMOC strength and its sensitivity to GIS melting, Swingedouw et al. (2009) reported that the background climate state is important for the AMOC's sensitivity and that the response is not linear with the freshwater forcing. This has been previously investigated by Ganopolski and Rahmstorf (2001), who found the cooler glacial climate to be more sensitive to freshwater input than the warmer interglacial climate, partly because of the ice-albedo feedback involving sea ice and the position of deep convection sites. Indeed, palaeoclimatological reconstructions provide strong evidence for higher sensitivity of the AMOC under glacial conditions, instabilities (e.g., Bianchi and McCave 1999; Elliot et al. 2002; Rahmstorf 2002; Alley 2007; Srokosz et al. 2012) and abrupt shifts between different modes of operation (Rahmstorf 2002). An important question is whether climate models are sensitive enough to reproduce such abrupt behaviour (Valdes 2011). However, abrupt changes in the strength of the AMOC appear largely absent during interglacial periods, with the exception of a number of events during the early deglaciation phases of the interglacials (Alley et al. 1997; Lang et al. 2010; Irvali et al. 2012). All the above gives rise to the question whether we can relate past changes in GIS melt and AMOC strength to evaluate future scenarios.

We present a systematic investigation of changes in the AMOC's response in simulations covering different warmer than present-day background climates (Last Interglacial, Present Interglacial, Future) and different GIS melt scenarios (ranging between 0 and 100 % GIS mass loss), performed with a coupled global climate model. Indeed, estimates of GIS melt rates during the LIG and PIG (respectively 12.7 mSv at 125 kiloyear before present, hereafter ka BP; Van de Berg et al. 2011; up to 26 mSv at 9 ka BP, Pelletier 2004; Blaschek and Renssen 2012) suggest that these were within the middle to upper range of what is expected for the future (3–24 mSv by 2100 AD, scenario A1B, Meehl et al. 2007). We argue that, with the time dependence of Earth system's sensitivity in mind, our approach enables us to estimate to what extent future AMOC changes are going to be similar to past changes. To take into consideration the importance of the model-dependent AMOC sensitivity to freshwater forcing, we include three different model versions with different AMOC sensitivities (low, medium and high). In short, our objective is to quantify three different

aspects of the AMOC response to GIS melt: (1) characteristics of the warm background climate, related to the corresponding radiative forcing, (2) different magnitudes of GIS melt, and (3) different model sensitivities of the AMOC's response to a melt water perturbation. Investigating these aspects will enable us to assess the underlying question to what extent we can use past warm climates to infer the AMOC's response to future climate warming.

In the following we review the important features of our model (Sect. 2.1) and outline the experimental set-up in Sect. 2.2. In Sect. 2.3 we provide a description of the considered three time periods and the main characteristics of the simulated background climates. Section 3 presents the simulated AMOC characteristics, the role of sea-ice feedbacks and the discussion of the results and the context.

2 Methods

2.1 The model

We performed experiments with the Earth system model of intermediate complexity (EMIC) LOVECLIM (version 1.2; Goosse et al. 2010). We included the interactive atmospheric, oceanic, sea ice and land surface components, but disabled the dynamical ice sheet model. In our approach GIS melt rates are prescribed and therefore allows a systematic analysis of its impacts as well as a precise control of the forcing, which is harder or even impossible to achieve when using a dynamical ice sheet component in a coupled model set-up. The elevation and extent of the GIS are fixed at present-day conditions, therefore snow and liquid precipitation accumulated on the ice sheet will be drained back to the ocean. Consequently, we do not take into account the negative impact of AMOC weakening on the GIS melt rate or atmospheric changes due to a diminished ice sheet. It has been previously shown that feedbacks involve changes in sea-ice cover, precipitation patterns and atmospheric circulation (Lunt et al. 2004; Junge et al. 2005; Stone and Lunt 2013), which affect the GIS itself, but also its surroundings. Lunt et al. (2004) argue that due to the decreased orography and change in albedo, temperatures rise in Greenland and reduce the meridional temperature gradient resulting in a reduced meridional heat transport. Arguably this is not to be neglected. However, Junge et al. (2005) find the atmospheric resolution of a model to be an important criteria of the potential impacts of a lowered GIS. Therefore it is uncertain whether these effects are competing on the sensitivity of the AMOC to GIS melt or not. Future research including interactive ice sheets could address these uncertainties and their impact on AMOC stability. Here we introduce only key-aspects of the model and refer for more details and a discussion of the performance

of LOVECLIM under present-day, past and future forcings to Goosse et al. (2010).

The sea-ice-ocean component of LOVECLIM (CLIO3; Goosse and Fichefet 1999) is a free-surface ocean general circulation model with a horizontal resolution of 3×3 degrees latitude-longitude and 20 vertical levels, coupled to a sea-ice component (Fichefet and Maqueda 1997, 1999). The atmospheric component (ECBILT; Opsteegh et al. 1998) is a spectral T21, three-level quasi-geostrophic model coupled to a land-surface module that employs a bucket-type hydrological model for soil moisture and runoff. Global cloud cover is prescribed from climatological seasonal means at present-day (Rossow 1996). As a result of an overestimation of precipitation over the North Atlantic and the Arctic, a fixed precipitation correction (8.5 and 25 %) is applied that removes part of this freshwater and repositions it to the North Pacific, where precipitation is underestimated. The dynamical vegetation model is called VECODE (Brovkin et al. 2002) and simulates two plant-functional types, trees and grasses and desert as a dummy type. The climate sensitivity to a doubling of the atmospheric CO₂ concentration is 1.9 K after 1000 year (Goosse et al. 2010) in the default version of LOVECLIM (version 1.2; using its standard parameter set). This is just outside the lower end of the range found in global climate models (2.1–4.4 K, Meehl et al. 2007). The simulated deep ocean circulation in LOVECLIM compares reasonably well with other model results (Schmittner et al. 2005), with deep convection taking place in both the Nordic Seas and the Labrador Sea (Goosse et al. 2010) and a maximum of the overturning stream function in the North Atlantic at 27°N of 15.6 ± 2.2 Sv (compared to observations at similar latitude of 18.7 ± 2.1 Sv in Kanzow et al. 2010).

Like any other climate model, LOVECLIM has numerous parameters that can be tuned to represent parameterized processes. Loutre et al. (2011) present different parameter sets for the LOVECLIM model, producing different model versions that span the full range of CO₂ sensitivities as well as cover a broad range of sensitivities of the AMOC to freshwater forcing. Yet, all these model versions produce results for present-day climate that are consistent and within the uncertainty of observations (global mean temperature, AMOC strength, sea-ice extent as in the supplementary of Loutre et al. 2011). In a comparison of model results with recent sea-ice extent decreases, the low sensitivity version was rejected by Goosse et al. (2007), because the sea-ice response was too slow. In this study we consider it as the lower range sensitivity. We use two of their alternative parameter sets that correspond to model versions that are more (high) or less sensitive (low) to freshwater forcing compared to the standard version (medium), but have almost the same CO₂ sensitivity. The corresponding naming in Loutre et al. (2011) is 112 for the less sensitive

Table 1 Summary of forcings in control and freshwater experiments

	Period	Name	Initial conditions	Radiative forcing anomaly (W/m ²)		
				Global	65°N	GHG
				Annual	Max	
Insolation values (Wm ⁻²) are global annual weighted mean radiative forcings and 65°N maxima, calculated from Huybers (2006) daily insolation data. GHG radiative forcing is calculated after IPCC (2001) formulation (reference values for 1750 AD)	Future	PI	Orbital (0 BP), PRE2005 1850 to 1950 AD	0.00	0.51	0.51
		RCP85	PI + RCP85 (2100 AD)	0.00	0.00	8.09
		RCP6	PI + RCP6 (2100 AD)	0.00	0.00	5.57
		RCP3	PI + RCP3 (2100 AD)	0.00	0.00	2.74
Present interglacial	PIG	Orbital (7 ka BP), Greenhouse gases from PMIP	0.22	31.98	-0.44	
Last interglacial	LIG	Orbital (128 ka BP), Greenhouse gases from PMIP	0.80	75.19	-0.06	

version and 222 for the more sensitive version. The differences in parameter values compared with the standard parameter set are shown in Table SI.1 and are summarized as follows. There are common differences of the low and the high parameter set compared to the medium, such as a higher sensitivity to greenhouse gases (up to +0.42 K) and a reduced Gent-McWilliams thickness diffusion coefficient, but also individual differences of each version that mark its characteristics. In the low version a major change is the lower diffusivity of the ocean compared to the medium and the high version, whereas in the high version an important change is a lower precipitation correction in the North Atlantic, resulting in a fresher surface ocean there. A simplified overview of the differences of the parameter sets and the impact on the sensitivity to greenhouse gas changes and sensitivity to freshwater forcing can be found in Fig.SI.1 and more information is provided by Loutre et al. (2011).

2.2 Experiment set-up

With the three versions of our model (low, medium and high) we performed quasi-equilibrium simulations for two past warm periods (Last and early Present Interglacial) and three future cases that are based on the 2100 AD values of the so-called Representative Concentration Pathways (RCP3, RCP6 and RCP85 as in Meinshausen et al. 2011), with 9 different GIS melt fluxes for each of these periods. The total number of simulations is thus 135 ($3 \times 5 \times 9$), with 27 for the Last Interglacial (LIG), 27 for the early Present Interglacial (PIG) and 81 for three future cases. Initial conditions for the snapshot experiments were spun up for 2000 model years to reach quasi-equilibrium conditions in all components of our model to applied forcings (cf. Renssen et al., 2006). The individual simulations have a duration of 500 model years with constant forcings. Although the duration of the simulations should ideally be about 1000 years to ensure quasi-equilibrium in all model components, this was not feasible given the computational expense this large number of simulations would require.

However, we argue that 500 years of simulation are sufficient to provide a reasonable estimate of equilibrium climate sensitivity. We forced all palaeoclimate simulations with orbital and greenhouse-gas concentrations in line with the PMIP3 protocol (<http://pmip3.lscce.ipsl.fr>). An overview of the simulations and their forcings is presented in Table 1.

The nine GIS melt scenarios consist of one control simulation with fixed orbital and greenhouse gases and eight GIS melt water scenarios that represent the melting of different percentages of the present-day GIS volume (2.911.080 km³) over a period of 500 years. These percentages are: 5, 10, 20, 30, 40, 50, 75 and 100 %. These ice volumes are converted to a melt flux as they are equally distributed over 500 years of model simulation, e.g. 5 % (145.554 km³) per 500 years \sim 9 mSv. The melt water is added as additional runoff to the existing runoff from Greenland (precipitation and snow melt) that is distributed to the oceans around Greenland as is illustrated in Bakker et al. (2012).

2.3 Periods: background climate

We chose our different time periods because they all resemble warm periods in the past or potentially in the future and in order to compare them with one another, we focus on the radiative forcing as a measure of how warm a certain climate was or is going to be. Past periods are forced by orbitally-induced insolation changes, but in near-future warm climates these are negligible compared to the radiative forcing induced by greenhouse gas emissions. Thus a first obvious distinction can be made between future and past climates on the basis of the radiative forcing. Here we introduce the three periods and provide the first results concerning the background climate state.

2.3.1 The last interglacial

The last interglacial lasted from about 130 to 115 ka BP. Its thermal maximum is recorded as one of the warmest periods

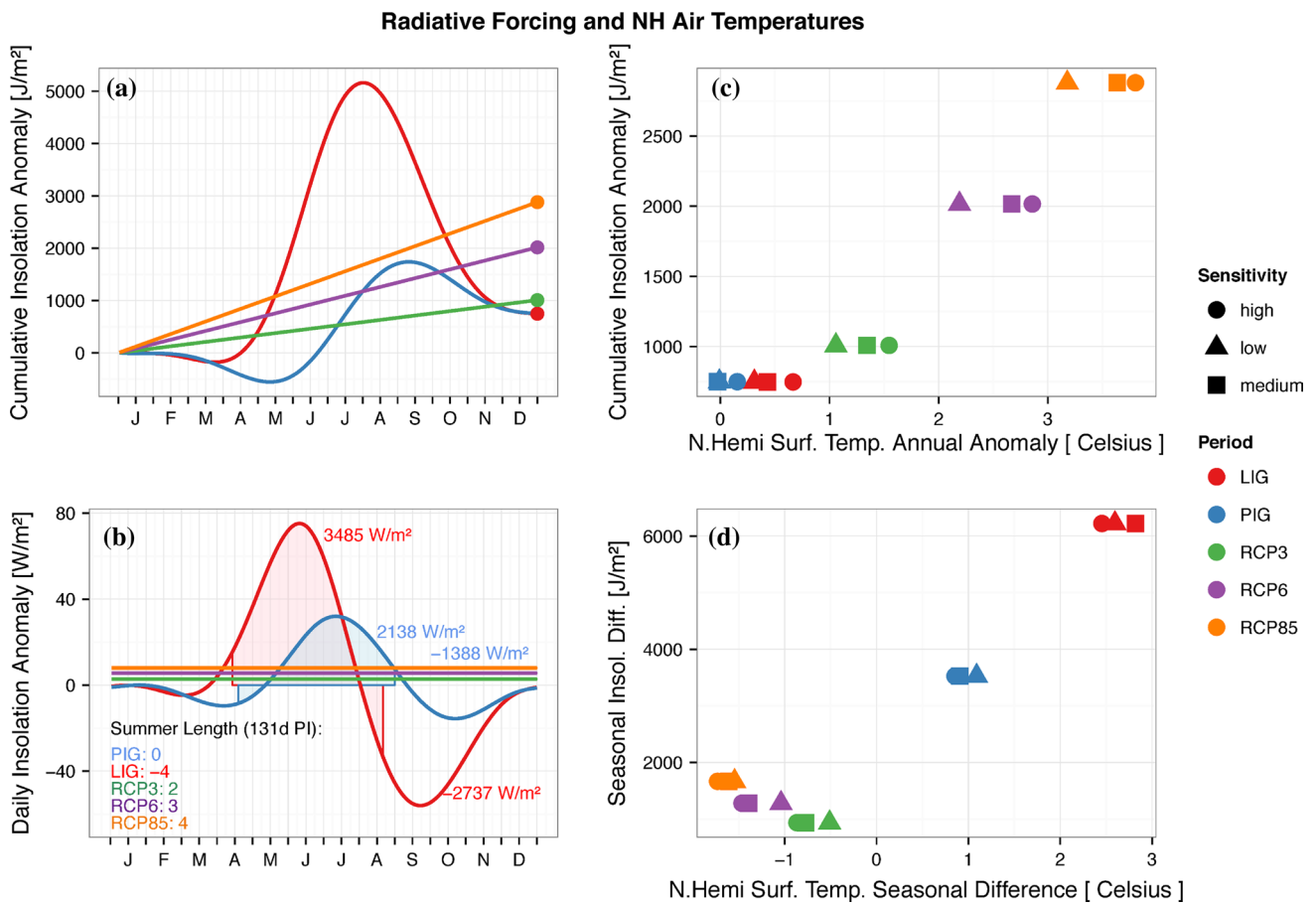


Fig. 1 Comparison of insolation anomalies and background climate states. **a** Cumulative insolation anomalies over the year (Jm^{-2}), representing the annual radiative forcing input at $65^{\circ}N$. **b** Cumulative insolation anomalies (Jm^{-2}) and Northern Hemisphere ($0-90^{\circ}N$) annual surface temperature anomalies. **c** The daily insolation anomaly and season length anomaly in days for $65^{\circ}N$, defined as the days of

the year with more than $300 Wm^{-2}$ insolation, representing the equilibrium temperature of a black body at $0^{\circ}C$ (as in Huybers 2006). *Shaded area* is the summer season radiative forcing for the LIG and FIG. **d** The seasonal insolation difference (SID) compared to the seasonal difference in Northern Hemisphere surface air temperature anomalies

during the last 250,000 years (CAPE Members 2006). We have chosen 128 ka BP as our time slice because it corresponds to the timing of the maximum orbitally-forced insolation anomaly during summer in the Northern Hemisphere ($+75 W/m^2$ at $65^{\circ}N$ compared to present-day, Fig. 1c; Huybers 2006), potentially leading to highest melting of the GIS. Van de Berg et al. (2011) showed that, in a regional climate model coupled to an ice sheet model, 45 % of the GIS melt is directly related to insolation and 55 % to the ambient temperature change. The contribution of GIS mass loss to the sea-level peak (6.6–8.4 m, Kopp et al. 2009; 2–4 m Dutton and Lambeck 2012) in the last interglacial has been recently confined to about 2 m (Dahl-Jensen et al. 2013), which represents approximately 30 % volume loss compared to the present-day ice volume (Tarasov and Peltier 2003; Overpeck et al. 2006). However the exact value remains uncertain and is within the range of 1.4–4.3 m (Robinson et al. 2011; Helsen et al. 2013; Stone and Lunt 2013). Last interglacial

reconstructions of GIS melt and ice-berg discharge yield about $12.7 \pm 0.1 mSv$ ($\sim 400 Gt/year$ at 125 ka BP, van de Berg et al. 2011) and are likely to have increased as the ice sheet lowered. In our last interglacial equilibrium control simulations (LIG, low to high) the Northern Hemisphere annual surface air temperatures are 0.3–0.7 K higher than at present day (Fig. 1b) and the seasonal temperature difference, as defined by the annual range of monthly means, is 2.4–2.8 K higher than at present-day (Fig. 1d). The increase in seasonality is mostly due to an increase in summer temperatures (1.8–2.1 K), whereas Fig. 1c shows as well lower insolation during early winter ($-56 Wm^{-2}$) and a 4 day shorter summer season. We define the summer season by the period during which daily insolation is above $300 Wm^{-2}$, which corresponds to an equilibrium temperature of $0^{\circ}C$ at $65^{\circ}N$ as in Huybers (2006). This allows a dynamical definition of summer and winter half year as the length and starting point of the seasons are allowed to change over time.

2.3.2 *The present interglacial: the Holocene thermal maximum*

The present interglacial started at 11.7 ka BP and experienced an orbitally-induced summer insolation maximum at about 10 ka BP (Berger and Loutre 1991). However the timing of the warmest part of the present interglacial, the so-called Holocene Thermal Maximum, was delayed relative to the insolation maximum over large parts of the Northern Hemisphere to 7–5 ka BP. This delay was caused by the impact of remnants of the Laurentide Ice Sheet (LIS, Renssen et al. 2009) and related melt fluxes into the Atlantic Ocean. To circumvent such complexities we decided not to include remnant ice sheets and use 7 ka BP conditions, a period with a positive orbitally-induced insolation anomaly of $+32 \text{ Wm}^{-2}$ at 65°N (Fig. 1c; Huybers 2006) and still considerable GIS melt. Early Present Interglacial GIS melt fluxes can be inferred from ice thickness changes from Peltier's ICE5G model that is constrained by sea-level reconstructions and glacioeustatic adjustment, resulting in values ranging between 3 and 26 mSv (in the period of 9–7 ka BP; Peltier 2004; Blaschek and Renssen 2013). Other modelled estimates have been summarized in Funder et al. (2011; cf. Fleming and Lambeck 2004; Simpson et al. 2009) and indicate a clear early Holocene retreat of the GIS, with contributions of up to 1.8 m of relative sea level from 10 to 7 ka BP. The minimum extent of the GIS was probably reached around 5 ka BP at the latest (Funder et al. 2011). In our present interglacial equilibrium control simulations (PIG, low to high) the Northern Hemisphere annual surface air temperatures are 0–0.15 K warmer than at present-day (Fig. 1b), and the seasonal temperature ranges are 0.8–1.1 K larger than at present-day (Fig. 1d). The increase in seasonality is mostly due to increased summer temperatures ($\sim 0.7 \text{ K}$), since Fig. 1c shows a small spring (-10 Wm^{-2}) and autumn (-16 Wm^{-2}) insolation anomaly minimum.

2.3.3 *The future: representative concentration pathways*

The Future scenarios are based on the Representative Concentration Pathways (RCP) from Meinshausen et al. (2011) and represent fixed greenhouse-gas concentrations at 2100 AD from RCP3, RCP6 and RCP85. To keep our approach simple and straightforward, we applied only changes of anthropogenic induced radiative forcing from greenhouse-gas concentrations. This forcing accounts for the majority of future anthropogenic induced changes (cf. Table 1) and represent a slightly reduced anthropogenic radiative forcing compared to the full emission scenarios presented by Meinshausen et al. (2011). The corresponding radiative forcing at 2100 AD is 2.7 Wm^{-2} for RCP3, 5.6 Wm^{-2} for RCP6 and 8 Wm^{-2} for RCP85. Note that, in our simulations we

investigate the equilibrium response rather than the transient response, which is lagging the forcing. In our future equilibrium control simulations (RCP3, RCP6, RCP8, low to high) the Northern Hemisphere annual surface air temperatures are 1.1–3.8 K warmer than at present-day (Fig. 1b). We find that the seasonal temperature range decreases by 0.5–1.7 K (Fig. 1d), because winter temperatures rise stronger (1.2–4.4 K) than summer temperatures (0.7–2.6 K). Consequently, the summer season becomes longer as well (2–4 days, Fig. 1c). Connected to the temperature rise is the predicted contribution of future GIS melt to sea-level rise in the range of 0.03–0.21 m per century, translating to a melt flux of about 3–24 mSv (Meehl et al. 2007) in addition to a present-day flux of $22.2 \pm 0.1 \text{ mSv}$ (van de Berg et al. 2011; 18 mSv in Dickson et al. 2007 for pre-industrial). These predictions can be considered conservative, as recent increases in GIS melt rate (Rignot et al. 2011; Bamber et al. 2012) suggest that this continuing trend will lead to near-future GIS melt rates that are likely to exceed previous projections (Meehl et al. 2007). Previous studies, such as Ridley et al. (2005), suggested a peak rate of 60 mSv in the early phase of a 3000 year long complete retreat of the GIS under increasing greenhouse-gas forcing. Overall the GIS will become a major contributor to future sea level rise (Rignot et al. 2011) and is likely an important source of freshwater in the North Atlantic region.

2.3.4 *Comparison of past and future climates*

In order to compare the three periods (LIG, PIG, future) we show in Fig. 1 the radiative forcing from daily insolation data (Huybers 2006) at 65°N and radiative forcing from greenhouse-gas emissions for the future cases (Table 1). The cumulative insolation anomaly (defined as the integrated insolation from January to December) in Fig. 1a shows that the LIG and the PIG have strong positive summer insolation anomalies compared to present day (cf. Fig. 1c), but also negative anomalies in spring and autumn. Therefore, accumulated over a whole year, LIG and PIG insolation anomalies add up to about 750 Jm^{-2} (here we neglect PIG and LIG greenhouse-gas changes), but for the future cases, greenhouse-gases induced radiative forcing anomalies add up to much higher yearly sums (1008 Jm^{-2} for RCP3, 2016 Jm^{-2} for RCP6 and 2880 Jm^{-2} for RCP85). When we compare the annual insolation accumulation with annual mean Northern Hemisphere surface air temperatures, we find a consistent pattern (Fig. 1b), indicating that more annual cumulative radiation forcing leads to higher annual Northern Hemisphere temperatures in our model. One has to keep in mind that this is particularly true for higher Northern latitudes, as past orbital insolation values varied substantially per latitude. On the one hand, it is possible that the annually warmer climates are

less freshwater sensitive climates in line with previous findings of Ganopolski and Rahmstorf (2001). On the other hand, we have shown that the past climates are characterized by larger seasonal ranges in both insolation (Fig. 1c) and temperature (Fig. 1d), whereas for future climates we find reduced seasonal ranges. Arguably, seasonality is relevant to the strength of the AMOC because cooler winter temperatures result in more suitable conditions for both convection in deep water formation areas and more sea-ice formation. Relevant in this context are both the severity of winter cooling and the duration of the period with cold temperatures that are closely linked to orbital insolation for the past climates (Fig. 1c). On the one hand, cooler winter temperatures allow sea ice to grow faster and foster convection by brine rejection, while on the other hand, expanded sea ice might be shielding the ocean from the atmosphere and thus reducing convective activity. However, despite these local effects of sea ice and convection, transport of freshwater from outside the vicinity of the convection area by increased sea-ice expansion would result in more surface freshening and stratification in the convection area, thus reducing convection and bringing that convection site closer to a collapse. This transport of freshwater would result from the sea ice melting during summer and winter transport of sea ice. This may indicate, therefore, that in climates with a larger seasonal contrast, such as the LIG and PIG, the AMOC could be more sensitive to freshwater forcing. Both interpretations, the annual and the seasonal, as well as the two mechanisms, the sea ice shielding convection and more freshwater being transported into convection areas, are valid at this point and it is in the next section, that we shall discuss this together with results of the AMOC strength.

Note that in the LOVECLIM model, the spring equinox is fixed to the 21st of March, which impacts the definition of monthly means used in our comparison to daily insolation data (Fig. 1d, e.g. further information in Joussaume and Braconnot 1997). Our monthly model output includes this bias whereas our dynamic definition of the seasons based on daily insolation, allowing them to shift inside the year, does not. Note that we apply GIS melt water throughout the year without seasonal differences. Recently Hu et al. (2011) described a minor difference in AMOC strength between simulations with annual and summer only GIS melt forcing. However, in a study using the same LOVECLIM model, Bakker et al. (2013a) did not find any notable impact of seasonality.

3 Results and discussion

We will first discuss our results in terms of impact of the background climate state on the unperturbed AMOC

strength (Sect. 3.1), and continue with the impact of GIS melt on the AMOC strength and the importance of model parameter sets (Sect. 3.2), then we take a more detailed look at the mechanisms involved in Sect. 3.3 and finally we discuss our results in context of climate sensitivity in Sect. 3.4.

3.1 AMOC state in the background climates

The AMOC strength in the unperturbed background climates is relevant for our estimation of its sensitivity to GIS melt water. We find that the mean AMOC strength (14 ± 1.6 Sv) at 27°N differs more by parameter set (1.4–2.5 Sv differences within one climate) than by time period (0.6–1 Sv differences per parameter set), with the strongest circulation in the low parameter set (15.9 Sv) and the weakest in the high parameter set (12.5 Sv, Fig. 2a). The early PIG is mostly the strongest within the range of simulations (~ 14.8 Sv) and the LIG the weakest (~ 13 Sv). The latter shows a particular minimum in our high parameter set, which is potentially linked to the strong decrease in summer sea-ice extent in the Arctic (Fig. 2b). However, it is uncertain whether the unperturbed strength of the AMOC was stronger or weaker during the early LIG (Born et al. 2011; Bakker et al. 2013b). The mean AMOC strength is dependent on the parameter set showing a decrease with higher freshwater sensitivity, however the variability within each parameter set remains similar. Convection from the surface to the deep ocean depends mainly on the buoyancy of the surface waters and the stability of the water column itself. Impacts from salt fluxes, precipitation, evaporation, temperature and sea ice affect convection at these convection areas and are thus relevant for the AMOC in total. Seasonal changes in sea-ice extent (error bars in Fig. 2b) are large for all simulations, however the largest for the LIG ($\sim 13.2 \times 10^{12}$ km²). The salt flux at 30°S northward in the Atlantic Ocean (Fig. 1c) indicates that in the future scenarios the salt import is higher compared to PIG and LIG and that a large difference exists between the high sensitivity version and the other parameter sets. The combined impacts are visible in the sea surface densities (SSD) in the North Atlantic ($90\text{--}30^\circ\text{W}$, $35\text{--}90^\circ\text{N}$, Fig. 1d). In the future scenarios SSDs are mostly lower compared to LIG and PIG. The highest densities are found in the PIG, and the lowest in RCP85. The lower SSDs in the future scenarios show that, despite higher salt import into the North Atlantic, SSDs are decreasing due to lower sea-ice area, higher temperatures and a more negative E–P balance (not shown). Despite these differences, the presence of convection (reaching more than 200 m depth) at the three major convection sites (Nordic Seas, Labrador Sea and around Iceland; Fig. SI.3) and the relatively similar AMOC strength in all unperturbed background climates suggests, that the

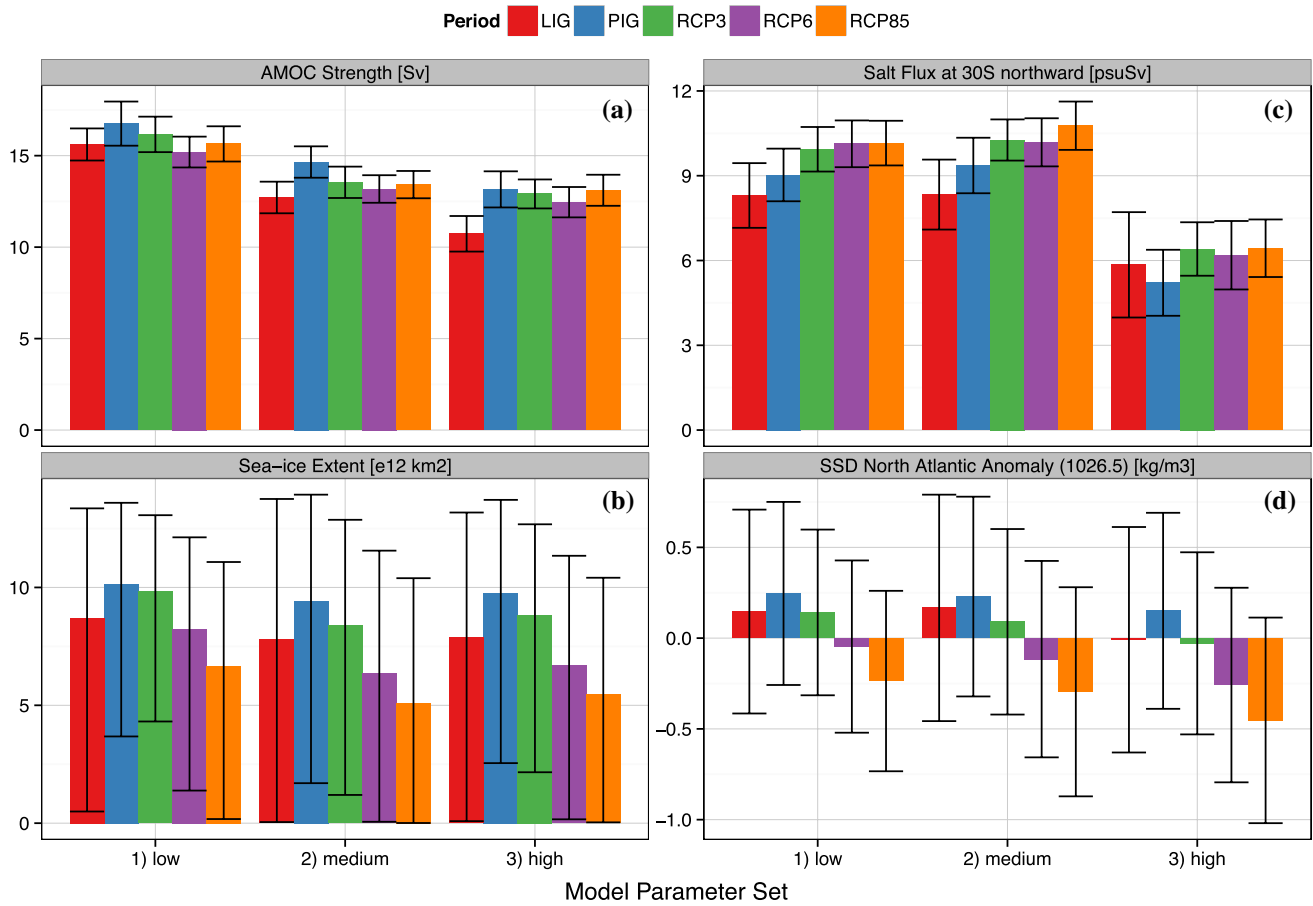


Fig. 2 Comparison of the background climate state showing the mean unperturbed AMOC strength (**a**) in Sv, as well as the standard deviation, and the mean sea-ice extent of the Northern Hemisphere in km² (**b**), as well as the minimum and maximum of the sea-ice extent. **c** Shows the salt inflow at 30°S in the North Atlantic northward in

psuSv and the standard deviation. **d** Shows the sea surface density in the North Atlantic (90–30°W, 35–90°N) as anomaly to 1,026.5 kg/m³ to show the changes more clearly. Values have been calculated over the last 100 years of each simulation

AMOC state in the background climate is of minor importance for the sensitivity of the AMOC to GIS melt water.

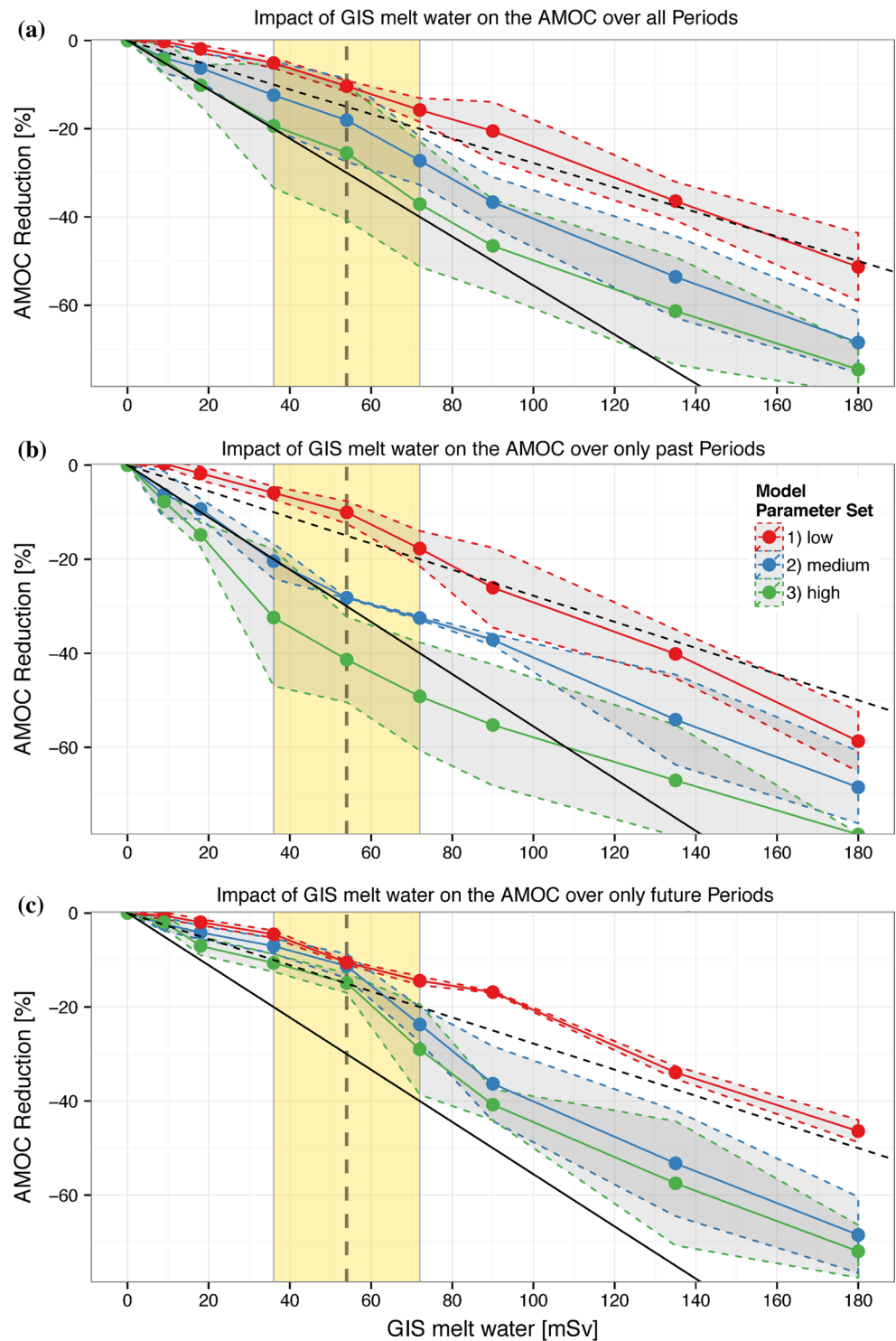
3.2 Impact of freshwater forcing on the AMOC strength

In Sect. 2.3 we have summarized forcings and temperatures of our control experiments for each period and found that there is a difference between past and future climates that originates from their forcings. Therefore we have decided to look more into the differences of past and future climates, rather than at each simulation separately. Individual results are available as supplementary information (Fig. SI.2).

The results show (Fig. 3a) that the relative AMOC sensitivity (size of anomaly relative to control) to freshwater forcing depends strongly on the used model parameter set. As expected, our three model versions diverge into a more (medium, high) and a less (low) sensitive configuration that is consistent over all time periods and suggests that parameter changes are very relevant to the results and implications

deduced. We will discuss this result in more detail in Sect. 4 and focus now on the differences of past and future climates per model parameter set. From Fig. 3b–c it is apparent that the difference in AMOC sensitivity to GIS melt between past and future is not constant, but changes as a function of the imposed GIS melt. This difference arrives at a maximum at 54 mSv GIS melt in the medium and high sensitivity parameter sets, before the difference decreases again with higher melt rates (Fig. 4a). The slopes of past AMOC changes for the medium and the high sensitivity parameter sets are steeper than their future counterparts before 54 mSv (Fig. 4b), weaker between 72 and 90 mSv and relatively similar at higher GIS melt rates. The difference between past and future, and the change of slope are both relevant for the interpretation, but do not provide a single melt rate value. Therefore, we define a transition zone from 36 to 72 mSv. This zone marks the transition in the AMOC response in past and future climates: with GIS melt rates lower than 36 mSv, the past and future climates respond very

Fig. 3 Summary of the AMOC changes due to GIS freshwater forcing per model realization. All panels show percentages of AMOC reduction and GIS melt water flux in mSv. **a** All simulations, past and future ones. **b** Only past simulations, LIG and PIG. **c** Only future simulations, RCP3, RCP6 and RCP85. Values are taken from 27°N and have been calculated over the last 100 years of each simulation and the percentages are presented as anomalies compared to the control simulation for each parameter set and period. The changes depicted by the percentages represent the AMOC's sensitivity to freshwater forcing. For individual simulations and absolute values of AMOC strength we refer to the SI. The shaded bands represent one standard deviation around the corresponding means. The area between 36 and 72 mSv is denoted as the transition zone and the *black dashed line* (at 54 mSv) indicates the maximum difference of past and future AMOC changes, as shown in Fig. 4. Solid black line (10 % AMOC reduction vs. 18 mSv GIS melt) and dashed black line (5 % AMOC reduction vs. 18 mSv GIS melt) give lines of constant AMOC sensitivity for reference



differently, while above 72 mSv they respond rather similarly. This transition zone is not valid for the low-sensitivity version of our model that hardly shows these differences between past and future climates, as well as slope changes (Fig. 4b). The changes in response of the AMOC to GIS melt water is not unlike a separation that has been reported by Bakker et al. (2012) with the same model in different

LIG GIS melting scenarios. They made a separation into three regimes (0–39 mSv, 52–130 mSv, 143–300 mSv) of AMOC response to GIS melt water. However the distinction between regimes was based on the shutdown of convection areas and sea-ice extent using a finer GIS melt stepping to distinguish between regimes, which are potentially hidden as we have less simulations with high melt rates.

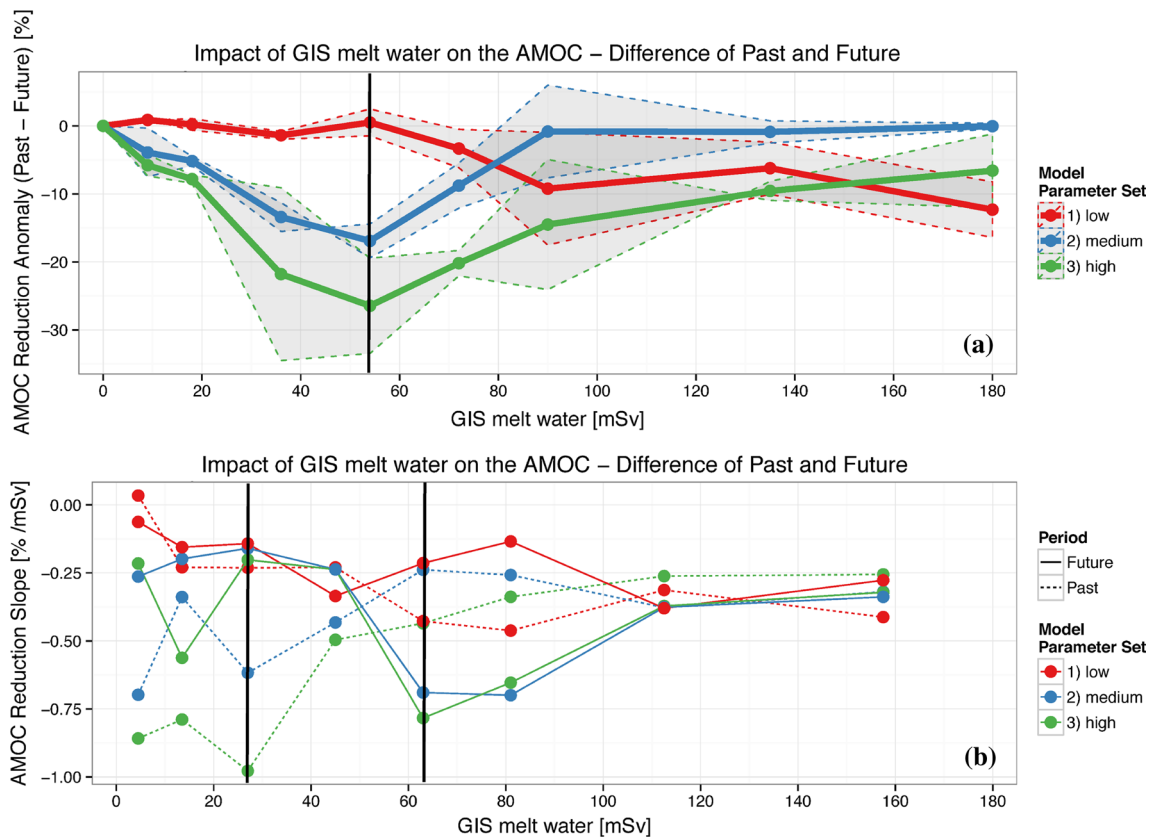


Fig. 4 AMOC response to GIS melting per model parameter set, shown as difference between past and future scenarios (a) and slopes of AMOC changes for past and future climates (b). Black lines indi-

cate the transition zone as in Fig. 3. Values used for the calculation of slopes and differences are shown in Fig. 3

Nevertheless a difference is visible in the lower GIS melt ranges in Figs. 3b–c or 4a between the future scenarios and the past climates, suggesting that the future climates change within the transition zone from being less sensitive to more sensitive with higher melt rates and come closer to the past climates. When we look at the absolute values of AMOC strength then the picture shifts a bit, because the periods and especially the model parameter sets have different mean values (Fig. 2, low: 15.9 Sv, medium: 13.5 Sv, high: 12.5 Sv, all time periods) and impacts differ especially for the past periods (Fig. SI.2). Nonetheless, the similarity between the medium and the high version remains. Differences in the absolute values of AMOC strength indicate primarily differences in the parameter sets, such as the initial value of AMOC strength or how large the differences are between the different periods. We find that the high parameter set produces absolute values that are much lower for LIG and PIG compared to the future scenarios. In the medium set this is not the case. When using the high sensitive version, the LIG simulation remains below all other simulations, independent of melt rates. In accordance with Swingedouw et al. (2009), this shows already the importance of the background climate on the AMOC state and its sensitivity to GIS

melt. When we consider for a moment that the low parameter set produces the same sensitivity to freshwater forcing in all climates investigated (Fig. 3), then the absolute values (Fig. SI.2) tell us that this is even possible with different mean values of AMOC strength. For the high version we find that the most sensitive time periods (LIG, PIG) are also the time periods with the weakest initial AMOC strength before perturbation with freshwater (Fig. 2a). As expected the medium version gives us an intermediate picture that shows weaker reductions compared to the high version, but still distinguishes between past and future climates.

The change in response to freshwater forcing within the transition zone seems to be linked to the actual setting and the background climate state of the different time periods. We can see in Fig. 4b that in the lower GIS melt range the past climates (PIG and LIG) are more sensitive compared to the future scenarios for both the medium and the high parameter sets. We have previously shown that Northern Hemisphere annual mean surface air temperatures align well with annual cumulative insolation forcing (Fig. 1b) and that applying these results to the sensitivity of the AMOC to GIS melt water suggests that the AMOC is more sensitive in climates with less annual mean insolation, such

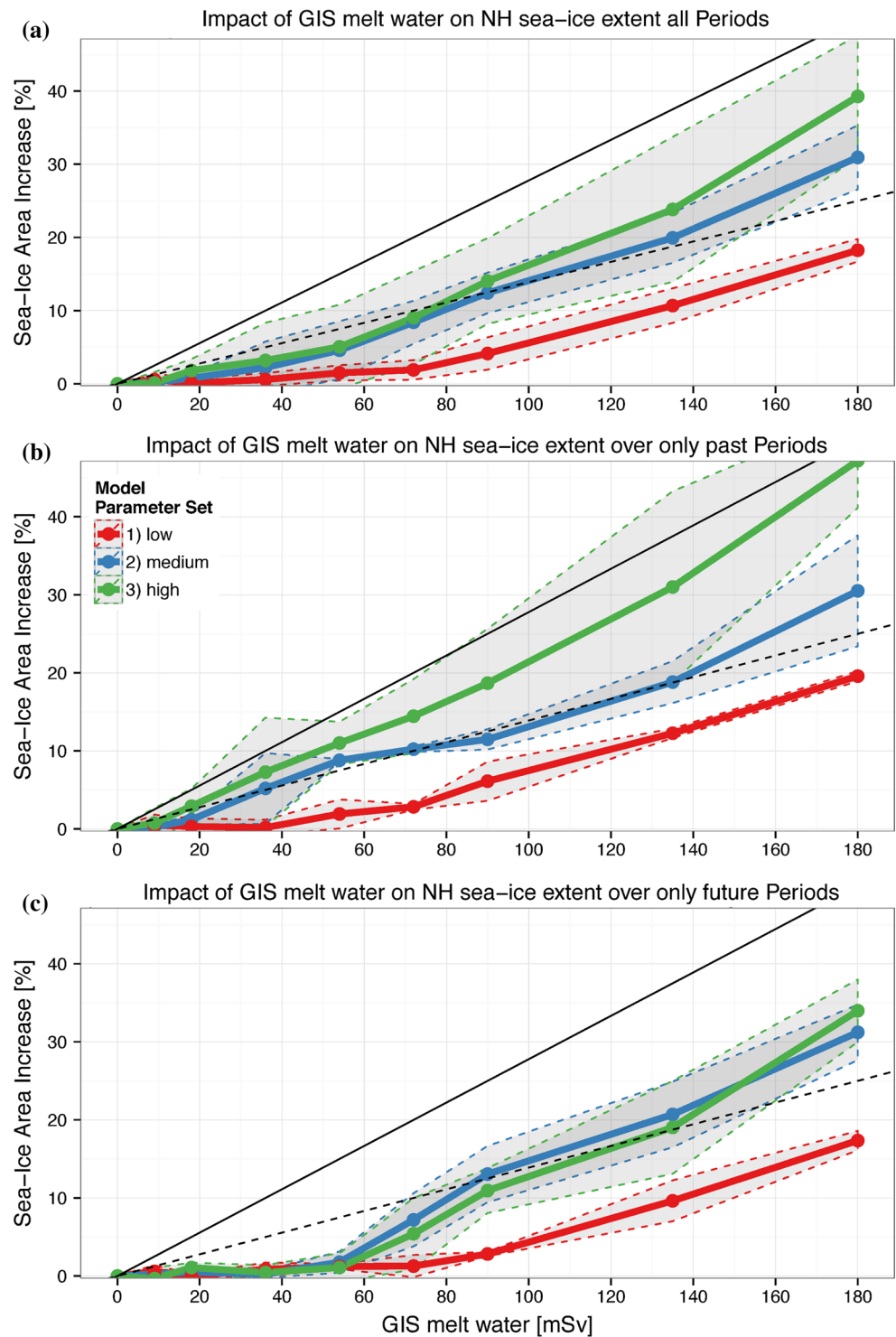
as the LIG and PIG. This interpretation is in general agreement with Swingedouw et al. (2009), however they also found that the response of the convection sites to freshwater forcing is critical in combination with the sea-ice cover. Therefore it is not unlikely that both the seasonal (Fig. 1c) and annual mean insolation forcing are relevant for the AMOC sensitivity to freshwater forcing. A potential explanation for a connection to mean annual forcing could be the energy distribution in the climate system, making transport processes relatively more important, thus the climate system more sensitive to disruption, such as to GIS melt water slowing down the AMOC. Applied to, for example the LGM, a cooler climate with a higher meridional temperature gradient (e.g. Shakun and Carlson 2010), depends more on the transport of heat from the tropics to the poles, thus resulting in a more sensitive AMOC to freshwater forcing (Swingedouw et al. 2009). However this relationship between AMOC sensitivity and annual mean forcing does not explain why the warmer future climates become more sensitive with higher GIS melt rates compared to past climates (cf. Fig. 3b–c), suggesting a dynamic response. We have reported on the seasonality of the forcing for LIG and PIG (Sect. 2.2), which implies cooler (-0.1 to -0.8 K) and longer winters (in LIG 4 days). In the model, these conditions lead to an increase in sea-ice cover (Fig. 2b). In a comparison between Northern Hemisphere seasonal surface air temperature differences and seasonal insolation difference (SID, Fig. 1d), we find that the future cases show the opposite response relative to the past climates. LIG and PIG show larger seasonal temperature differences, whereas in the future cases the difference decreases as the result of higher winter temperatures. The results suggest that not only the Northern Hemisphere annual mean temperatures are important, but that the seasonality of the background state is relevant for the strength of the AMOC, as climates with higher seasonality seem to be more sensitive to freshwater forcing as can be seen in Fig. 3b, lower GIS melt range. However, from seasonal temperatures or insolation forcing alone, it is not possible to explain why future cases become more sensitive above 54 mSv GIS melt (Fig. 3c). Therefore we will analyse in the following section the impact of changes in seasonality on winter convection and sea-ice cover in the convection areas and its dependency on the amount of GIS melt water.

3.3 Convective activity and sea-ice feedback

Connected by the strong cooling during winter, convection and sea ice formation are seasonal processes that interact with each other and make it hard to distinguish between feedback and forcing. Nevertheless we find in Fig. 5 (sea ice extent anomaly compared to control), a difference that corresponds well with the separation made in

Fig. 3. Before 54 mSv GIS melt, the future scenarios have hardly any sea-ice feedback (Fig. 5c), compared to the past climates (Fig. 5b) in the medium and high sensitivity parameter sets. In order to connect better to the convection areas and analyse the different response in the lower and the higher GIS melt range, we take two example GIS melt scenarios, one at 36 mSv (20 % GIS mass loss) and one at 135 mSv (75 % GIS mass loss), and the corresponding control simulation. Furthermore, we focus only on LIG, PIG and RCP6, because RCP3 and RCP85 show minimal differences in convection depth and sea-ice margin patterns compared to RCP6 and only for the medium model parameter set. The maps show absolute annual sea surface salinities (SSS) for the control simulations (Fig. 6, column 1) and anomalies for the freshwater perturbed simulations (columns 2 and 3), as well as winter maximum and summer minimum sea-ice extent and winter maximum convection layer depth as black contours. For the control simulation, results show some differences between different time periods mostly South of Denmark Strait. For example, this area is in the LIG and RCP6 much fresher compared to the PIG most likely related to a more southern sea-ice extent and related melting during summer. Convective activity can be found in the Labrador Sea (LS), Around Iceland (AI), such as in the Irminger Sea, and in the Norwegian Sea (NS). In the control simulations convection is active in all regions (Fig. 6, black contours). Once we added 36 mSv of GIS melt water (Fig. 6, column 2), the LIG has no convection and an enhanced sea-ice extent in the LS compared to PIG and RCP6. The freshening signal in SSS in LS is much more expressed in the LIG compared to PIG or RCP6 given the same amount of GIS melt. In the PIG and RCP6, LS convection remains active, though reduced. However, the response and spatial pattern of freshening is quite different between the three periods. In the PIG the centre of freshening is close to the Denmark Strait, reducing convection and expanding sea ice to the tip of Greenland. In the LIG the freshening is centred on the West Coast of Greenland in the LS, shutting down convection there and covering the LS with sea ice. In RCP6 the surface freshening is weakest compared to the past periods with a centre close to the tip of Greenland and weaker impacts on convective activity (Fig. 3c) and minor changes in sea-ice extent. The sea-ice extent, the amount of freshening and the corresponding location of active convection characterize some of the differences between the past climates and the future cases. Major differences between PIG and LIG are the freshening in the LS and the maximum and minimum sea-ice extent, as the Arctic becomes almost ice-free at the end of summer in the LIG. At this point it seems clear that the LS and the origin of this extended freshening in the LS is key in explaining the different response seen in Fig. 3 between past and future climates. We continue with the higher GIS

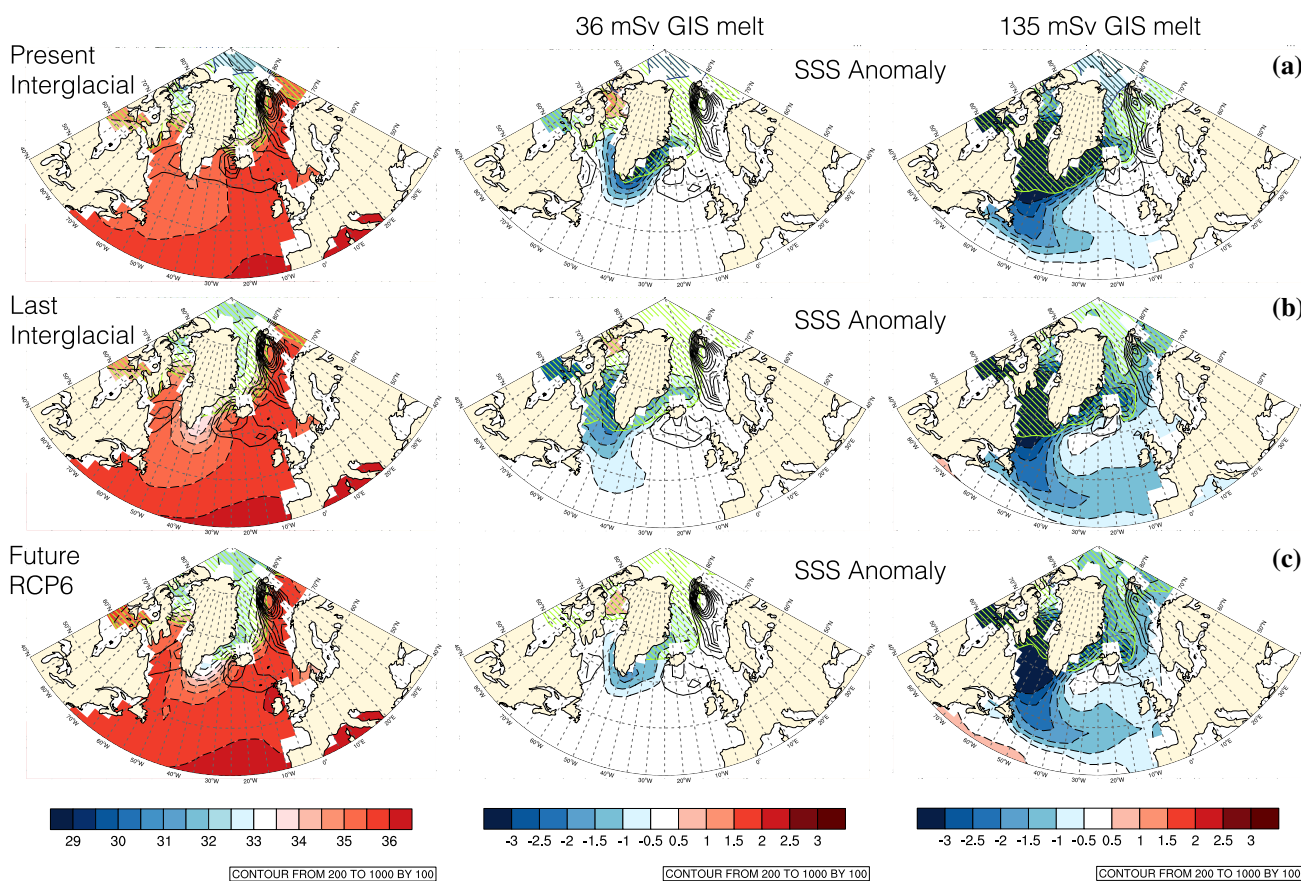
Fig. 5 Summary of the sea-ice area response to GIS melting per model parameter set. All panels show percentages of sea-ice cover change and GIS melt water flux in mSv. **a** All simulations, past and future ones. **b** Only past simulations, LIG and PIG. **c** Only future simulations, RCP3, RCP6 and RCP85. Values give Northern Hemisphere sea-ice cover over the last 100 years of each simulation and the percentages are presented as anomalies compared to the control simulation for each parameter set and period. *Solid black line* (5 % sea-ice cover change vs. 18 mSv GIS melt) and *dashed black line* (5 % sea-ice cover change vs. 9 mSv GIS melt) give lines of constant sea-ice cover change for reference



melt simulations before we focus more on convection in the LS.

In our simulations with a higher GIS melt flux (135 mSv; Fig. 6, column 3) we find a relatively similar picture for all periods (LIG, PIG, RCP6) in terms of surface freshening of the North Atlantic, but a different one for the past climates (LIG, PIG) and RCP6 in terms of sea-ice extent.

Convective activity is reduced in all convection areas and no LS convection is present in any of the presented simulations (cf. Fig. 7a). AMOC reductions in Fig. 3 indicate that past climates are relatively close together and share almost the same sea-ice extent (Figs. 5, 6a–b). While the sea-ice advance in RCP6 is different compared to the PIG, convective activity is comparable except for a slight weakening



Annual mean SSS [p.s.u.] (filled), winter maximum/summer minimum sea-ice extent [1] (color contours) & convection layer depth [m] (black solid contours)

Fig. 6 Convection areas and sea-ice margin for the control simulations, 36 mSv or 20 % and 135 mSv or 75 % GIS melt. Maps show annual sea surface salinities (SSS), winter maximum convection depth (m) as well as winter maximum (green striped) and summer

minimum (blue striped) sea-ice extent (described by the lead fraction above 15 %) over the last 100 years of each simulation considering the medium sensitivity version of our model. **a** Simulations of the PIG, **b** Simulations of the LIG, **c** Simulations of RCP6

in NS in RCP6. A detailed analysis of each melt case (cf. Fig. 7a and Fig.SI.3) suggests that LS is the most sensitive convection region in terms of freshwater needed to inhibit convection there. Beyond a certain amount of GIS melt, the LS becomes sea ice covered for the past climates and stratified in the future cases (Fig. 7b). This result is independent of model realization. Whereas this higher sensitivity exists in the past climates at different GIS melt rates, LIG 36 mSv and PIG 54 mSv, in the future scenarios this seems to be missing. However as we have seen in Fig. 6 a major difference between LIG and PIG is the freshening of LS as well as extensive sea-ice cover. At this point it is unclear whether surface freshening or sea-ice cover shielding convective activity in the LS in the LIG is more relevant, as the leading and lagging of the two processes is hard to distinguish. However, in combination with results seen in Fig. 7, we find that in the PIG just a bit more GIS melt water is needed to give a similar response in the LS.

This thus suggests, that the amount of freshening in the LS is different between the two climates. Vertical profiles in the Labrador Sea (Fig. 8) exhibit more stratification in the LIG compared to any other model simulation and support the idea that indeed surface freshening is more relevant as opposed to sea-ice cover shielding convection. Indicated by the advancing sea-ice cover towards the tip of Greenland in Fig. 6a in the PIG, it seems likely that the expansion of sea-ice acts as a freshwater transport to the South and into the LS. This additional freshening causes LS convection to collapse at lower GIS melt rates in the LIG compared to the PIG and RCP6.

The response seen in Fig. 3 between the past and future simulations is clearly impacted by the circumstances in the LS, but as well by the activities in the other convection areas. Convective activity around Iceland is rather robust and again relatively independent of the model parameter set. Related to a weakening of convection in LS, the AI

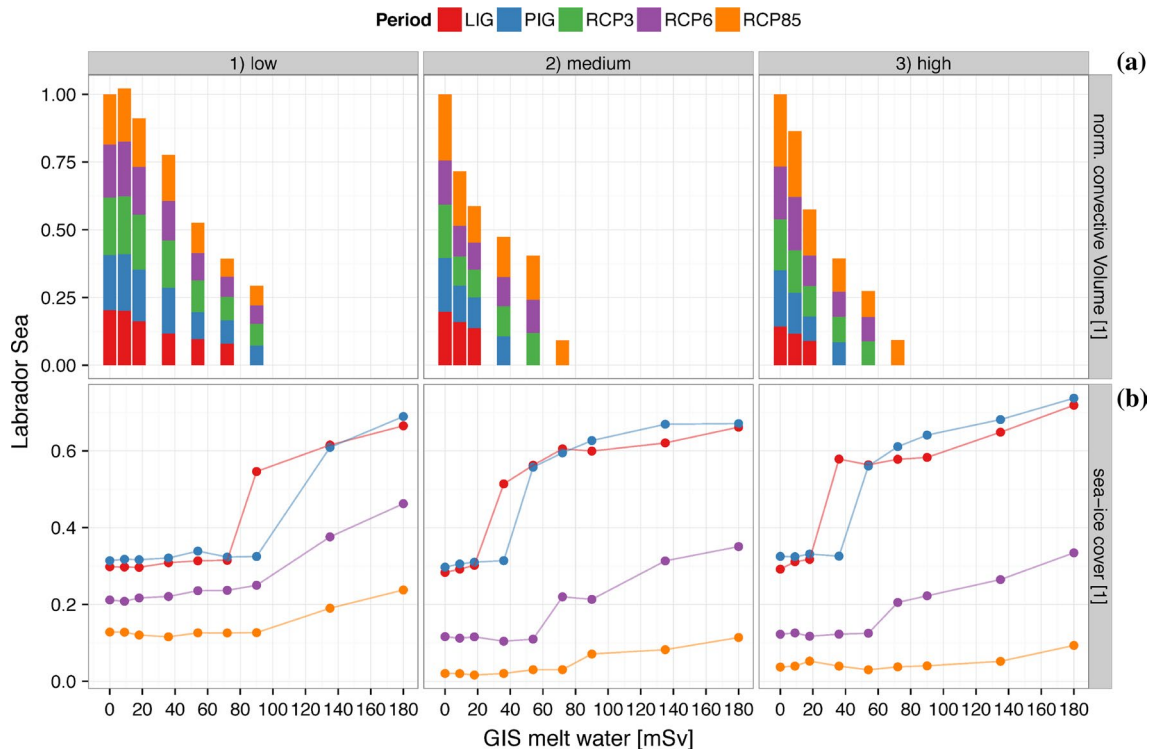


Fig. 7 Labrador Sea normalized convective volume resembling convection activity and sea-ice cover. **a** Normalized convective volume, that is calculated using the convective layer depth (above 200 m) multiplied by the area and then normalized using the unperturbed vol-

ume (with total volume of all 5 experiments being 1.0). Additional information in Fig.SI.3. **b** Annual mean sea-ice cover. The values are calculated from the last 100 years of each simulation in the Labrador Sea (LS, 90–45°W, 50–70°N)

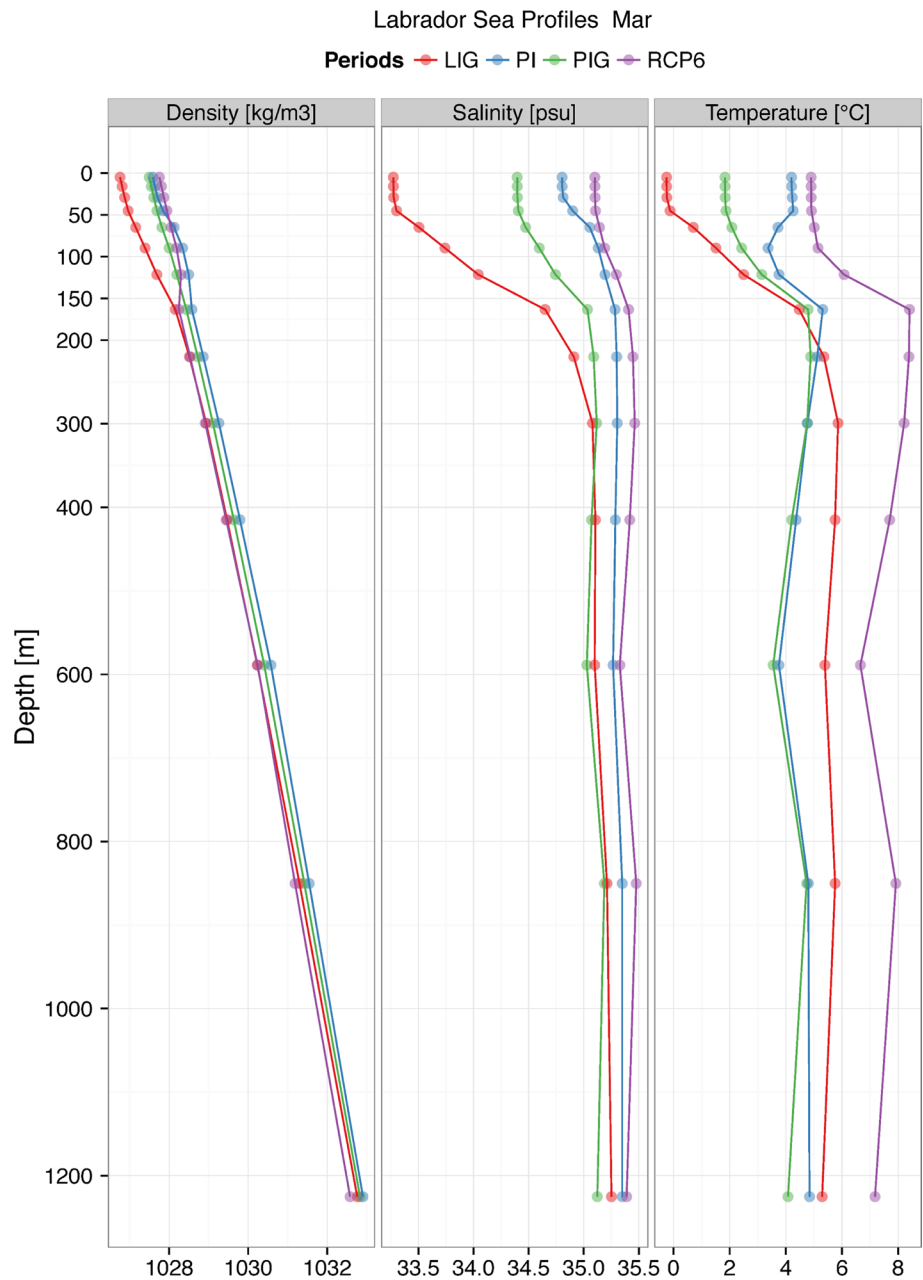
strength increases as a result of a shift of convection outside LS and sea-ice related cooling and advection of relatively cooler air. Therefore a slight increase in convective activity in all simulations can be seen in AI. However, the biggest changes can be seen in the NS in terms of model parameter set, time period and GIS melt flux. The NS convection region, the most important convection site in our model, is found just southwest of Svalbard, so relatively close to the sea-ice edge. This makes this region, on one hand, prone to advancing sea ice that can hamper ocean-atmosphere heat exchange, but on the other hand, resistant because of the low temperatures at this extremely northern position. Medium and high model parameter sets show both a considerable decrease of convection depth in NS with high GIS melt rates, in agreement with results from Fig. 3. Whereas for lower GIS melt rates all model versions give weak increases in convection layer depth in NS, potentially related to decreases of other convection sites and the overall increase of sea ice and related cooling.

Summarizing, for the past warm periods we find that the different response of the AMOC in the lower GIS melt range relates to the convective activity in the convection areas (as summarized in Fig. 7a, the North

Atlantic) and the seasonal cycle of sea-ice formation and melt (Fig. 7b). The response of the sea-ice expansion due to GIS melting depends on the climatic conditions of the background climate and it is only in such cases when the expansion of sea ice reaches far enough to affect convection in the LS, that a different response in AMOC strength can be found. In the future scenarios, this sea-ice response and transport of freshwater into the LS is only a minor process, most likely because of higher winter temperatures (up to 4.4 K in RCP8.5, Sect. 2.3) and subsequent smaller expansion of sea ice (Fig. 5c). At higher GIS melt rates the stratification of the ocean surface inhibits or weakens convection at different convection sites, resulting in cooling and sea-ice expansion and reduced AMOC values alike (Fig. 3b–c). However, there are still important differences between the periods. For example, in the future scenarios at higher GIS melt rates, the LS is stratified, rather than covered by sea ice as in the LIG or the PIG (Fig. 6c), whereas the NS convection site is impacted by both freshening and sea-ice cover in all climates alike.

Other mechanisms that have been suggested to explain differences in the AMOC sensitivity to melt water input are discussed in the next section.

Fig. 8 March Labrador Sea vertical profiles of density, temperature and salinity. Simulations LIG, PIG and RCP6 include 36 mSv of GIS melt water as seen in Fig. 6, simulation PI represents a pre-industrial reference simulation that does not include additional GIS melt water. All model simulation values have been calculated from the last 100 years of each simulation in the Labrador Sea (LS, 90–45°W, 50–70°N)

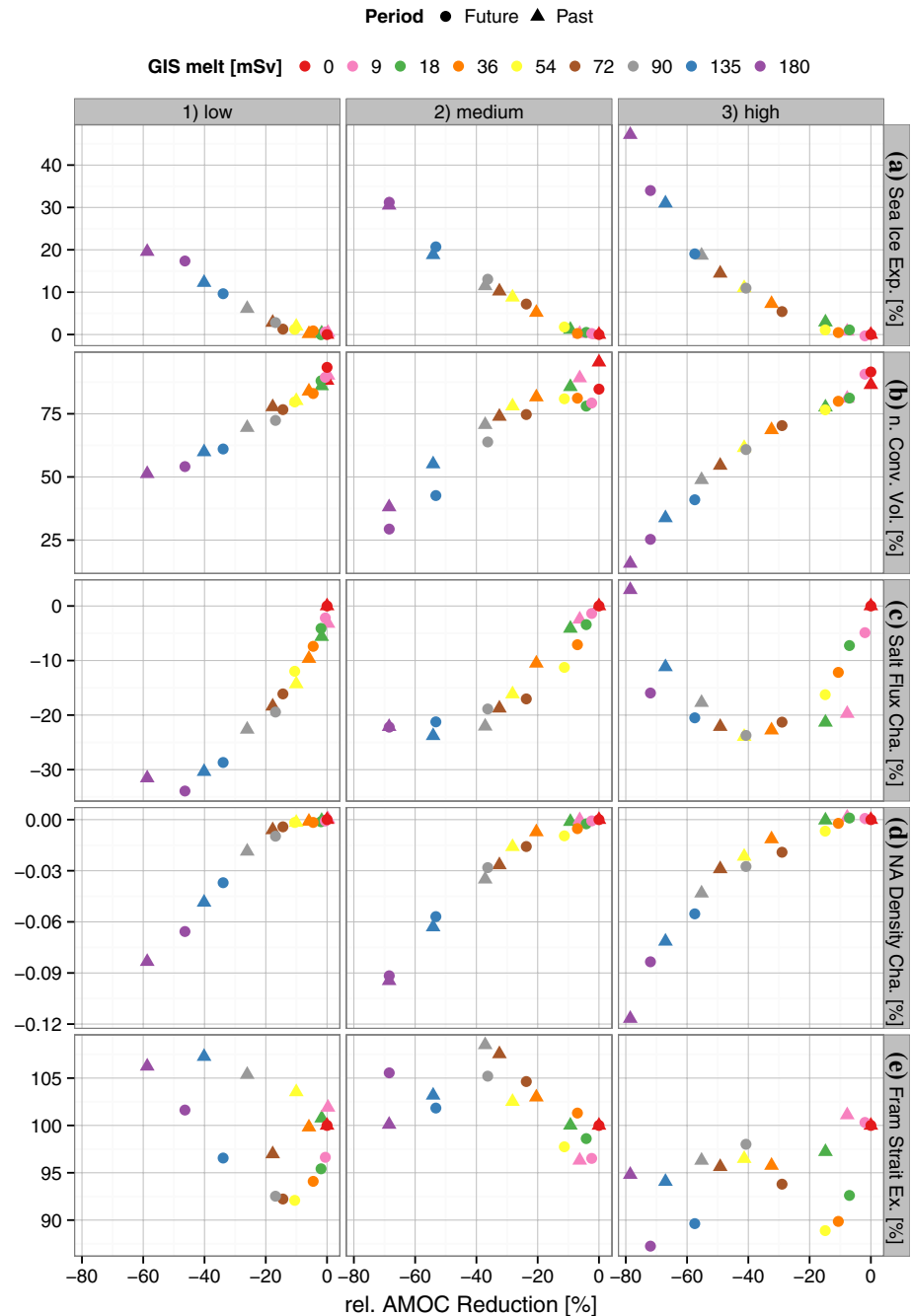


4 Discussion and context

The comparison of past and future AMOC sensitivity can be done on the basis of annual mean insolation, or radiative forcing for future emission scenarios respectively, and yield higher values for climates that have less forcing. We argue that this is related to the fact that cooler climates depend stronger on the heat transport northward, as has been previously shown by Swingedouw et al. (2009). However our results also show, that future climates can become more sensitive to higher GIS melt (Fig. 3c), hence it is more likely that a dynamic feedback interacts with the GIS melt water and the AMOC. We find the sea-ice response in past

and future climates to be different just like the response of the AMOC to GIS melting (Fig. 5) in the lower GIS melt range. Our results further show that this different response is caused mainly by the sensitivity of the LS convection site to freshwater entering the LS, thus the amount of freshening. The transport of freshwater by the sea-ice expansion into the LS brings convection there closer to a collapse and modifies the overall response to a given GIS melt rate. The expansion of sea ice is most likely driven locally by surface cooling and freshwater stratifying the surface ocean as well as globally by the heat transport and the seasonality of the climate. Not unlikely, but inconclusive is the idea that changes in Fram Strait sea-ice export (Fig. 9e) could

Fig. 9 Scatterplot of relevant variables compared to AMOC reduction to GIS melt water for past and future simulations and per model parameter set. **a** Northern Hemisphere sea–ice area, as anomaly compared to the control simulation, as in Fig. 5. **b** North Atlantic normalized convective volume, as in Fig. SI.3. **c** Salt flux at 30°S northward in the North Atlantic, as anomaly compared to the control simulation, as in Fig. 2c. **d** Sea surface density of the North Atlantic as anomaly compared to the control simulation, as in Fig. 2d. **e** Fram Strait sea–ice export as anomaly compared to the control simulations



cause the reported sea-ice expansion and highlight the Arctic Ocean as the source of this different response. Modeling results give weak changes (5–10 %) but large inter-annual variability (30 %).

Other studies (Rahmstorf 1996; Latif et al. 2000; Swingedouw et al. 2007) have shown that the salt import into the North Atlantic is crucial for the stability of convection and the AMOC sensitivity to melt water forcing. Our results agree with this interpretation to some extent, as the salt import into the North Atlantic (Fig. 7c) relates as well to the AMOC strength. However, SSDs for the unperturbed

states (Fig. 2d) are lower in the future scenarios and decrease even further with higher GIS melt rates (Fig. 7d). Increased inflow of salty waters in the future scenarios is counteracted by more local sea-ice melting and surface warming, yielding lower SSDs in the convection areas (Fig. SI.4). Therefore, it is reasonable to argue that this stabilizing effect (Rahmstorf 1996; Latif et al. 2000; Swingedouw et al. 2007) is not the main mechanism that controls the difference between past (LIG, PIG) and future (RCP3, RCP6, RCP85) AMOC sensitivity in the lower GIS melt ranges. The difference in sea-ice expansion, freshwater transport

and its interaction with convection, most prominently in the LS, allows explaining this difference in AMOC response to GIS melting. Ultimately this difference lies in the seasonality of the climate, which determines the amount of sea ice formation and modifies the oceanic response to a land-based ice sheet melting.

To better understand how future climate change compares with changes that occurred in past warm periods, we have investigated the relationship between the background climate state, the AMOC's strength and GIS melt. We have systematically analysed the sensitivity of the AMOC to freshwater forcing from the GIS and found that the model parameter set, which describes mainly the sensitivity of the model to freshwater forcing, plays a major role in determining what consequences can be expected from using past reconstructions in future predictions. If we consider a freshwater-sensitive parameter set, our results suggest that, at lower GIS melt rates (less than 54 mSv), the relation between the AMOC and GIS melt differs considerably between past and future warm periods. However, they are very similar when a parameter set with lower freshwater sensitivity is used. Unfortunately there is little constraint on the sensitivity of the AMOC to freshwater forcing in the real world. Nonetheless, in two out of three cases (medium, high) impacts on past climates are different from future ones in terms of ocean circulation. This could imply that the differences in the seasonal distribution of the radiative forcing make past climates very different from present and future climates in terms of convection depth and sea-ice feedback and therewith the overall AMOC response.

Climate sensitivity describes the response of global temperatures to changes in global radiation modified by numerous feedbacks from all components of the climate system. Our primary interest is the AMOC as a feedback and whether our climate-related AMOC sensitivity in the lower GIS melt range is impacting global climate sensitivity. An estimation of climate sensitivity (defined as the annual mean global temperature change divided by the radiative forcing) in all our future cases, including all GIS melting scenarios, yields relatively constant values per parameter set (0.39, 0.42, 0.51 K/Wm⁻² for low, medium and high parameter sets), varying weakly (0.04 K/Wm⁻²) by emission scenario or GIS melt. This near constancy of the climate sensitivity in the future scenarios is a result of the relatively large simulated global warming of 1–4 K compared to an up to 0.6 K decrease due to GIS melting (depending on parameter set). The stronger impacts are found in the weaker warming scenarios and in the medium to high parameter sets. The melting of the GIS weakens the AMOC and therewith the northward transport of heat and causes an expansion of the sea-ice cover, resulting in global cooling. Similar temperature impacts of 0.7 K (LIG) to 0.9 K (PIG) due to GIS melting are found in the past

simulations. Due to the relatively small magnitude of the annual mean warming (LIG: 0.5 K, PIG: 0.2 K) it is in the same order of magnitude with the cooling. However, following the methodology of climate sensitivity to compare global annual mean temperatures with global annual mean radiation changes, we find that for our past warm climates the corresponding climate sensitivity varies strongly as a function of GIS melt amount and AMOC strength (–1 to +3 K/Wm⁻²). Furthermore, we find that the GIS melt related reductions in global temperatures are consistently larger, even though the differences are relatively small, in the past simulations compared to the future scenarios, mainly caused by stronger feedbacks related to the Arctic sea-ice cover in the past climates (e.g., ice-albedo and ice-insulation feedbacks). The application of the climate sensitivity concept to small annual forcings (LIG, PIG) has to be seen with caution. Firstly, it can be argued that in climates, such as the future, that are strongly forced by changes in greenhouse gases, the feedback from a GIS-melt-reduced AMOC on climate sensitivity can be regarded as of only minor importance within the 500 year of our experiment length. On longer time scales its importance can potentially be much larger. Secondly, our results indicate that it is not straightforward to use reconstructions of past warm climates that are characterised by changes in the seasonal forcing, such as the PIG and LIG, to infer the climate sensitivity of the future warm climate that is dominated by greenhouse-gas forcing.

Because of the seasonality in the orbital forcing, it has been argued (e.g. Zeebe 2013) that the Paleocene-Eocene Thermal Maximum (PETM) would be more suited to estimate climate sensitivity for future projections, because the PETM was also primarily greenhouse-gas driven. However the PETM (about 55 million years ago) is about 50 million years before glaciation in the Northern Hemisphere occurred making it unsuitable to study the feedback related to GIS melt. Another period sometimes referred to as a good analogue, in terms of insolation, is Marine Isotope Stage 11 because it had a similar seasonal distribution of insolation (Loutre and Berger 2003). However, there are some uncertainties concerning whether it was generally warmer (Milker et al. 2013) than present-day climate or not (Loutre and Berger 2003). Milker et al. (2013) indicate that regional differences are quite large, but on a global scale the surface ocean underwent deglacial warming in pace with CO₂ rise. However it is unlikely that there was a period that matched “anthropogenic” development exactly, including all boundary conditions, such as ice sheets. Therefore the problem of a correct analogue for future changes is very challenging and is accompanied by practical concerns about using data from periods so far back in time like data availability, uncertainties in the reconstructions and an overall lack of information about the boundary conditions in those climates.

Besides the discussion whether the early PIG and LIG are appropriate analogues for future changes, Valdes (2011) pointed out that the AMOC in the GCMs used for predictions of future warming, might not be sensitive enough to show abrupt changes such as cold stadial events recorded in the Greenland ice cores. However, according to our model experiments, the future AMOC is in two out of three cases less sensitive to GIS melt water than during the LIG and PIG, particularly because of reduced seasonal differences and winter warming. Our results partly suggest that future predictions are less impacted by freshwater sensitivity than the LIG and PIG, and that the insensitivity suggested by Valdes (2011) is thus possibly of less importance for future predictions. However, in our model this difference in sensitivity is mainly related to sea ice and Stroeve et al. (2007) found an overestimation of IPCC AR4 (2007) models and observed sea-ice cover over the last decades, that suggests, consistent with our results, that GCM's insensitivity is potentially related to sea-ice processes. This argumentation is supported by Goosse et al. (2007), who found that using different model parameter sets allowed a closer match to observed sea-ice extent. Their results suggest (based on a slightly different version of LOVECLIM and partly different parameter sets) that our least sensitive version (low; comparable to their parameter version E1) is likely to be too insensitive in terms of sea-ice response to recent reductions in sea-ice extent. Despite some differences between their parameter sets and ours, their findings suggest that the medium and high parameter sets are likely to result in a better representation of the climate. Therefore we argue that the AMOC's sensitivity to GIS melt found in the medium and high parameter set is more trustworthy than results of the low version.

The close relation of sea-ice formation and deep convection accounts for a large part for the higher sensitivity of the AMOC to GIS melt in past climates compared to the future. At present we cannot assess how important the low complexity and resolution of our model is in relation with sea-ice distribution and deep convection and therefore AMOC sensitivity. We thus encourage testing this result with higher complexity models, as the found threshold is model specific and is dependent on the physical approximations within a model. The parameterization of sub-grid processes such as convection or mixing is one example of that dependency, as observed values of these parameters are poorly known for the global ocean (Stone 2004). Dalan et al. (2005) report for an EMIC that varying the diapycnal mixing, a parameter crucial for the ocean circulation, modifies the freshwater sensitivity of the ocean circulation and changes the threshold for a shutdown of the thermohaline circulation. Therefore further testing could help us to better understand the parameterization of physical processes in our model that influence the interactions of convection and

sea-ice formation, as these interactions appear to be clearly different in past and future climate scenarios.

The future will be in many ways different from the past. Catastrophic cooling events as recorded in the past are unlikely to happen within the next century (Meehl et al. 2007), but the question on how long the warming will continue remains important. The role of slow feedbacks, such as the interaction between the GIS and the AMOC, are critical to long-term changes in the climate system.

5 Conclusions

We have systematically analysed the impact of various GIS melt rates on the AMOC strength in two past warm climates and three future warming cases, and with three different model parameter sets that yield different sensitivities of the AMOC to a freshwater perturbation.

Results with the two freshwater-sensitive model versions (medium and high) suggest:

The AMOC sensitivity to GIS melt can be separated into two GIS melt ranges.

- In the first GIS melt range (<54 mSv), the AMOC's sensitivity differs between past and future climates and thus depends on the background climate.
 - The high/low AMOC sensitivity in the past/future climates corresponds well with larger/smaller seasonal temperature ranges.
 - This difference in AMOC sensitivity between past and future climates is strongly dependent on the amount of freshwater being supplied to the Labrador Sea convection site. In climates with a stronger (past climates) or weaker (future climates) sea-ice expansion, more (past) or less (future) freshwater is being transported into the Labrador Sea, bringing the convection site closer to a local shutdown, given the same amount of GIS melting.
 - The increased freshwater transport by sea ice in the past climates compared to the future projections is a result of the enhanced seasonality. Both winter and summer temperatures act on the expansion of sea ice and the release of freshwater during summer.
 - Due to the difference of past and future AMOC sensitivity, it is likely that, for GIS melt fluxes <54 mSv, proxy-based reconstructions of past AMOC sensitivity will overestimate the importance of GIS melting if interpreted for future applications.
- In the second GIS melt range (>54 mSv), the AMOC's sensitivity is similar in all time periods investigated and thus independent of the background climate state.

- The sea–ice extent varies stronger between model parameter sets (low, medium and high) than between past and future climates.
- Proxy-based reconstructions of past AMOC sensitivity are likely to be applicable to future cases for GIS melt fluxes >54 mSv.

Results with the freshwater-insensitive version (low) suggest:

- The AMOC's sensitivity to GIS melt water is insensitive to the background climate state and the GIS melt water forcing.
- Proxy-based reconstructions of past AMOC sensitivity are likely to be applicable to future cases regardless of the applied GIS melt flux.
- However, the parameters in the low version are similar to a parameter set that was rejected by Goosse et al. (2007) for being too insensitive to simulate the observed recent decrease in sea-ice extent, rendering its predictions as less reliable for future interpretations.

Overall our results indicate that the AMOC's sensitivity in a model can be altered considerably by tuning its parameterized processes and that results are not independent of these choices. Furthermore, our results suggest that, in contrast to the past warm periods, the feedback from a GIS-melt-reduced AMOC has relatively little impact on future climate sensitivity because of the overwhelming GHG forced warming. However this can potentially change if the balance between the magnitude of the warming and the climate feedback changes on the long run.

MB and HR are supported by the funding of the European Community's 7th Framework Program (FP7/2007–2013), Marie-Curie Actions, under Grant Agreement No. 238111—CASE ITN. PB and HR are supported by the European Community's 7th Framework Program (FP7/2007–2013) under Grant Agreement No. 243908—“Past4Future. Climate change - Learning from the past climate”. This is Past4Future contribution No. 64. This support is gratefully acknowledged. We thank the anonymous reviewers and the editor for the constructive discussion and input to this manuscript.

References

- Alley RB (2007) Wally was right: predictive ability of the North Atlantic “conveyor belt” hypothesis for abrupt climate change. *Annu Rev Earth Planet Sci* 35:241–272. doi:10.1146/annurev.earth.35.081006.131524
- Alley RB, Mayewski PA, Sowers T et al (1997) Holocene climatic instability: a prominent, widespread event 8200 yr ago. *Geology* 25:483–486. doi:10.1130/0091-7613(1997)025<0483:HCIAPW>2.3.CO;2
- Bakker P, Van Meerbeek CJ, Renssen H (2012) Sensitivity of the North Atlantic climate to Greenland ice sheet melting during the Last Interglacial. *Clim Past* 8:995–1009. doi:10.5194/cp-8-995-2012
- Bakker P, Renssen H, Van Meerbeek CJ (2013a) Early last interglacial Greenland ice sheet melting and a sustained period of meridional overturning weakening: a model analysis of the uncertainties. *Clim Dyn* 1–15. doi:10.1007/s00382-013-1935-1
- Bakker P, Stone EJ, Charbit S et al (2013b) Last interglacial temperature evolution—a model inter-comparison. *Clim Past* 9:605–619. doi:10.5194/cp-9-605-2013
- Bamber J, van den Broeke M, Ettema J, Lenaerts J, Rignot E (2012) Recent large increases in freshwater fluxes from Greenland into the north atlantic. *Geophys Res Lett* 39(19):L19–L501. doi:10.1029/2012GL052552
- Berger A, Loutre M (1991) Insolation values for the climate of the last 10 million years. *Quat Sci Rev* 10(4):297–317. doi:10.1016/0277-3791(91)90033-Q
- Bianchi GG, McCave IN (1999) Holocene periodicity in North Atlantic climate and deep-ocean flow south of Iceland. *Nature* 397:515–517. doi:10.1038/17362
- Blaschek M, Renssen H (2013) The Holocene thermal maximum in the Nordic Seas: the impact of Greenland ice sheet melt and other forcings in a coupled atmosphere–sea–ice–ocean model. *Clim Past* 9:1629–1643. doi:10.5194/cp-9-1629-2013
- Born A, Nisancioglu KH, Risebrobakken B (2011) Late Eemian warming in the Nordic Seas as seen in proxy data and climate models. *Paleoceanography* 26:PA2207. doi:10.1029/2010PA002027
- Brovkin V et al (2002) Carbon cycle, vegetation, and climate dynamics in the Holocene: experiments with the CLIMBER-2 model. *Global Biogeochem Cycles*. doi:10.1029/2001GB001662
- Dahl-Jensen D, Albert MR, Aldahan A et al (2013) Eemian interglacial reconstructed from a Greenland folded ice core. *Nature* 493:489–494. doi:10.1038/nature11789
- Dalan F, Stone PH, Kamenkovich IV, Scott JR (2005) Sensitivity of the ocean's climate to diapycnal diffusivity in an EMIC. Part I: equilibrium State. *J Clim* 18:2460–2481. doi:10.1175/JCLI3411.1
- Dickson R, Rudels B, Dye S et al (2007) Current estimates of freshwater flux through Arctic and subarctic seas. *Prog Oceanogr* 73:210–230. doi:10.1016/j.pocean.2006.12.003
- Drijfhout SS, Hazeleger W (2006) Changes in MOC and gyre-induced Atlantic Ocean heat transport. *Geophys Res Lett* 33:n/a–n/a. doi:10.1029/2006GL025807
- Dutton A, Lambeck K (2012) Ice volume and sea level during the last interglacial. *Science* (80) 337:216. doi:10.1126/science.1205749
- Elliot M, Labeyrie L, Duplessy J-C (2002) Changes in North Atlantic deep-water formation associated with the Dansgaard-Oeschger temperature oscillations (60–10 ka). *Quat Sci Rev* 21:1153–1165. doi:10.1016/S0277-3791(01)00137-8
- Fichefet T (2003) Implications of changes in freshwater flux from the Greenland ice sheet for the climate of the 21st century. *Geophys Res Lett* 30:1911. doi:10.1029/2003GL017826
- Fichefet T, Maqueda MAM (1997) Sensitivity of a global sea ice model to the treatment of ice thermodynamics and dynamics. *J Geophys Res* 102:12609–12646
- Fichefet T, Maqueda MAM (1999) Modelling the influence of snow accumulation and snow–ice formation on the seasonal cycle of the Antarctic sea–ice cover. *Clim Dyn* 15:251–268
- Fleming K, Lambeck K (2004) Constraints on the Greenland ice sheet since the last glacial maximum from sea-level observations and glacial-rebound models. *Quat Sci Rev* 23:1053–1077. doi:10.1016/j.quascirev.2003.11.001
- Funder S, Goosse H, Jepsen H et al (2011) A 10,000-year record of Arctic Ocean sea–ice variability—view from the beach. *Science* 333:747–750. doi:10.1126/science.1202760

- Ganopolski A, Rahmstorf S (2001) Rapid changes of glacial climate simulated in a coupled climate model. *Nature* 409:153–158. doi:[10.1038/35051500](https://doi.org/10.1038/35051500)
- Goosse H, Fichefet T (1999) Importance of ice–ocean interactions for the global ocean circulation: a model study. *J Geophys Res* 104:23337. doi:[10.1029/1999JC900215](https://doi.org/10.1029/1999JC900215)
- Goosse H, Driesschaert E, Fichefet T, Loutre M-F (2007) Information on the early Holocene climate constrains the summer sea ice projections for the 21st century. *Clim Past* 3:683–692. doi:[10.5194/cp-3-683-2007](https://doi.org/10.5194/cp-3-683-2007)
- Goosse H, Brovkin V, Fichefet T et al (2010) Description of the earth system model of intermediate complexity LOVECLIM version 1.2. *Geosci Model Dev Discuss* 3:309–390. doi:[10.5194/gmdd-3-309-2010](https://doi.org/10.5194/gmdd-3-309-2010)
- Helsen MM, van de Berg WJ, van de Wal RSW et al (2013) Coupled regional climate—ice-sheet simulation shows limited Greenland ice loss during the Eemian. *Clim Past* 9:1773–1788. doi:[10.5194/cp-9-1773-2013](https://doi.org/10.5194/cp-9-1773-2013)
- Hofmann M, Rahmstorf S, Schellnhuber HJ (2009) On the stability of the Atlantic meridional overturning circulation. *Proc Natl Acad Sci USA* 106:20584–20589. doi:[10.1073/pnas.0909146106](https://doi.org/10.1073/pnas.0909146106)
- Hu A, Meehl GA, Han W, Yin J (2011) Effect of the potential melting of the Greenland ice sheet on the meridional overturning circulation and global climate in the future. *Deep Sea Res Part II Top Stud Oceanogr* 58:1914–1926. doi:[10.1016/j.dsr2.2010.10.069](https://doi.org/10.1016/j.dsr2.2010.10.069)
- Huybers P (2006) Early pleistocene glacial cycles and the integrated summer insolation forcing. *Science* 80(313):508–511. doi:[10.1126/science.1125249](https://doi.org/10.1126/science.1125249)
- Irvali N, Ninnemann US, Galaasen EV et al (2012) Rapid switches in subpolar North Atlantic hydrography and climate during the Last Interglacial (MIS 5e). *Paleoceanography*. doi:[10.1029/2011PA002244](https://doi.org/10.1029/2011PA002244)
- Johns WE, Baringer MO, Beal LM et al (2011) Continuous, array-based estimates of Atlantic ocean heat transport at 26.5 N. *J Clim* 24:2429–2449. doi:[10.1175/2010JCLI3997.1](https://doi.org/10.1175/2010JCLI3997.1)
- Joussaume S, Braconnot P (1997) Sensitivity of paleoclimate simulation results to season definitions. *J Geophys Res Atmos* 102:1943–1956. doi:[10.1029/96JD01989](https://doi.org/10.1029/96JD01989)
- Junge MM, Blender R, Fraedrich K et al (2005) A world without Greenland: impacts on the Northern hemisphere winter circulation in low- and high-resolution models. *Clim Dyn* 24:297–307. doi:[10.1007/s00382-004-0501-2](https://doi.org/10.1007/s00382-004-0501-2)
- Kanzow T, Cunningham SA, Johns WE et al (2010) Seasonal variability of the Atlantic meridional overturning circulation at 26.5 N. *J Clim* 23:5678–5698. doi:[10.1175/2010JCLI3389.1](https://doi.org/10.1175/2010JCLI3389.1)
- Köhler P, Bintanja R, Fischer H et al (2010) What caused Earth's temperature variations during the last 800,000 years? Data-based evidence on radiative forcing and constraints on climate sensitivity. *Quat Sci Rev* 29:129–145. doi:[10.1016/j.quascirev.2009.09.026](https://doi.org/10.1016/j.quascirev.2009.09.026)
- Kopp RE, Simons FJ, Mitrovica JX et al (2009) Probabilistic assessment of sea level during the last interglacial stage. *Nature* 462:863–867. doi:[10.1038/nature08686](https://doi.org/10.1038/nature08686)
- Kuhlbrodt T, Griesel A, Montoya M, Levermann A, Hofmann M, Rahmstorf S (2007) On the driving processes of the Atlantic meridional overturning circulation. *Rev Geophys* 45(2) doi:[10.1029/2004RG000166](https://doi.org/10.1029/2004RG000166)
- Lang B, Bedford A, Brooks SJ, Jones RT, Richardson N, Birks HJB, Marshall JD (2010) Early-holocene temperature variability inferred from chironomid assemblages at Hawes water, northwest England. *Holocene* 20(6):943–954. doi:[10.1177/0959683610366157](https://doi.org/10.1177/0959683610366157)
- Latif M, Roeckner E, Mikolajewicz U, Voss R (2000) Tropical stabilization of the thermohaline circulation in a greenhouse warming simulation. *J Clim*. doi:[10.1175/1520-0442\(2000\)013<1809:L>2.CO;2](https://doi.org/10.1175/1520-0442(2000)013<1809:L>2.CO;2)
- Loutre M, Berger A (2003) Marine isotope stage 11 as an analogue for the present interglacial. *Glob Planetary Change* 36(3):209–217. doi:[10.1016/S0921-8181\(02\)00186-8](https://doi.org/10.1016/S0921-8181(02)00186-8)
- Loutre MF, Mouchet A, Fichefet T et al (2011) Evaluating climate model performance with various parameter sets using observations over the recent past. *Clim Past* 7:511–526. doi:[10.5194/cp-7-511-2011](https://doi.org/10.5194/cp-7-511-2011)
- Lunt DJ, Noblet-Ducoudré N, Charbit S (2004) Effects of a melted Greenland ice sheet on climate, vegetation, and the cryosphere. *Clim Dyn* 23:679–694. doi:[10.1007/s00382-004-0463-4](https://doi.org/10.1007/s00382-004-0463-4)
- Lunt DJ, Haywood AM, Schmidt GA et al (2010) Earth system sensitivity inferred from Pliocene modelling and data. *Nat Geosci* 3:60–64. doi:[10.1038/ngeo706](https://doi.org/10.1038/ngeo706)
- Marshall J, Schott F (1999) Open-ocean convection: observations, theory, and models. *Rev Geophys* 37:1–64. doi:[10.1029/98RG02739](https://doi.org/10.1029/98RG02739)
- Meehl GA, Stocker TF, Collins WD et al (2007) Global climate projections. In: *Climate change 2007: The Physical Science Basis* Meinshausen M, Smith SJ, Calvin K et al (2011) The RCP greenhouse gas concentrations and their extensions from 1765 to 2300. *Clim Change* 109:213–241. doi:[10.1007/s10584-011-0156-z](https://doi.org/10.1007/s10584-011-0156-z)
- Members CAPE (2006) Last interglacial Arctic warmth confirms polar amplification of climate change. *Quat Sci Rev* 25:1383–1400. doi:[10.1016/j.quascirev.2006.01.033](https://doi.org/10.1016/j.quascirev.2006.01.033)
- Milker Y, Rachmayani R, Weinkauff MFG et al (2013) Global and regional sea surface temperature trends during Marine Isotope Stage 11. *Clim Past* 9:2231–2252. doi:[10.5194/cp-9-2231-2013](https://doi.org/10.5194/cp-9-2231-2013)
- Opsteegh JD, Haarsma RJ, Selten FM, Kattenberg A (1998) ECBILT: a dynamic alternative to mixed boundary conditions in ocean models. *Tellus A* 50:348–367. doi:[10.1034/j.1600-0870.1998.t01-1-00007.x](https://doi.org/10.1034/j.1600-0870.1998.t01-1-00007.x)
- Overpeck JT, Otto-Bliesner BL, Miller GH et al (2006) Paleoclimatic evidence for future ice-sheet instability and rapid sea-level rise. *Science* 311(5768):1747–1750. doi:[10.1126/science.1115159](https://doi.org/10.1126/science.1115159)
- Palaeosens Project Members, Rohling EJ, Sluijs A et al (2012) Making sense of palaeoclimate sensitivity. *Nature* 491:683–691. doi:[10.1038/nature11574](https://doi.org/10.1038/nature11574)
- Peltier WR (2004) Global glacial isostasy and the surface of the ice-age earth: the ICE-5G (VM2) model and grace. *Annu Rev Earth Planet Sci* 32:111–149. doi:[10.1146/annurev.earth.32.082503.144359](https://doi.org/10.1146/annurev.earth.32.082503.144359)
- Pickart RS, Spall MA, Ribergaard MH et al (2003) Deep convection in the Irminger Sea forced by the Greenland tip jet. *Nature* 424:152–156
- Rahmstorf S (1996) On the freshwater forcing and transport of the Atlantic thermohaline circulation. *Clim Dyn* 12:799–811. doi:[10.1007/s003820050144](https://doi.org/10.1007/s003820050144)
- Rahmstorf S (2002) Ocean circulation and climate during the past 120,000 years. *Nature* 419:207–214. doi:[10.1038/nature01090](https://doi.org/10.1038/nature01090)
- Renssen H, Goosse H, Muscheler R et al (2006) Coupled climate model simulation of Holocene cooling events: oceanic feedback amplifies solar forcing. *Clim Past* 2:79–90
- Renssen H, Seppä H, Heiri O et al (2009) The spatial and temporal complexity of the Holocene thermal maximum. *Nat Geosci* 2:411–414. doi:[10.1038/ngeo513](https://doi.org/10.1038/ngeo513)
- Ridley JK, Huybrechts P, Gregory JM, Lowe JA (2005) Elimination of the Greenland ice sheet in a High CO₂ Climate. *J Clim* 18:3409–3427. doi:[10.1175/JCLI3482.1](https://doi.org/10.1175/JCLI3482.1)
- Rignot E, Velicogna I, van den Broeke MR et al (2011) Acceleration of the contribution of the Greenland and Antarctic ice sheets to sea level rise. *Geophys Res Lett* 38:L05503. doi:[10.1029/2011JGL046583](https://doi.org/10.1029/2011JGL046583)
- Robinson A, Calov R, Ganopolski A (2011) Greenland ice sheet model parameters constrained using simulations of the Eemian interglacial. *Clim Past* 7:381–396. doi:[10.5194/cp-7-381-2011](https://doi.org/10.5194/cp-7-381-2011)
- Roe G (2009) Feedbacks, timescales, and seeing red. *Annu Rev Earth Planet Sci* 37:93–115. doi:[10.1146/annurev.earth.061008.134734](https://doi.org/10.1146/annurev.earth.061008.134734)
- Rossov WB (1996) International satellite cloud climatology project (ISCCP): documentation of new cloud datasets. NASA Goddard Space Flight Center

- Schmittner A, Latif M, Schneider B (2005) Model projections of the North Atlantic thermohaline circulation for the 21st century assessed by observations. *Geophys Res Lett* 32:L23710. doi:[10.1029/2005GL024368](https://doi.org/10.1029/2005GL024368)
- Schneider B, Latif M, Schmittner A (2007) Evaluation of different methods to assess model projections of the future evolution of the Atlantic meridional overturning circulation. *J Clim* 20:2121. doi:[10.1175/JCLI4128.1](https://doi.org/10.1175/JCLI4128.1)
- Shakun JD, Carlson AE (2010) A global perspective on last glacial maximum to Holocene climate change. *Quat Sci Rev* 29:1801–1816. doi:[10.1016/j.quascirev.2010.03.016](https://doi.org/10.1016/j.quascirev.2010.03.016)
- Simpson MJR, Milne GA, Huybrechts P, Long AJ (2009) Calibrating a glaciological model of the Greenland ice sheet from the Last Glacial Maximum to present-day using field observations of relative sea level and ice extent. *Quat Sci Rev* 28:1631–1657. doi:[10.1016/j.quascirev.2009.03.004](https://doi.org/10.1016/j.quascirev.2009.03.004)
- Srokosz M, Baringer M, Bryden H et al (2012) Past, present, and future changes in the Atlantic meridional overturning circulation. *Bull Am Meteorol Soc* 93:1663–1676. doi:[10.1175/BAMS-D-11-00151.1](https://doi.org/10.1175/BAMS-D-11-00151.1)
- Stone PH (2004) Climate prediction: the limits of ocean models. Washington DC Am Geophys Union Geophys Monogr Ser 150:259–267. doi:[10.1029/150GM20](https://doi.org/10.1029/150GM20)
- Stone E, Lunt D (2013) The role of vegetation feedbacks on Greenland glaciation. *Clim Dyn* 40:2671–2686. doi:[10.1007/s00382-012-1390-4](https://doi.org/10.1007/s00382-012-1390-4)
- Stouffer RJ, Yin J, Gregory JM et al (2006) Investigating the causes of the response of the thermohaline circulation to past and future climate changes. *J Clim* 19:1365–1387. doi:[10.1175/JCLI3689.1](https://doi.org/10.1175/JCLI3689.1)
- Stroeve J, Holland MM, Meier W et al (2007) Arctic sea ice decline: faster than forecast. *Geophys Res Lett*. doi:[10.1029/2007GL029703](https://doi.org/10.1029/2007GL029703)
- Swingedouw D, Braconnot P, Marti O (2006) Sensitivity of the Atlantic meridional overturning circulation to the melting from northern glaciers in climate change experiments. *Geophys Res Lett* 33:L07711. doi:[10.1029/2006GL025765](https://doi.org/10.1029/2006GL025765)
- Swingedouw D, Braconnot P, Delecluse P et al (2007) Quantifying the AMOC feedbacks during a $2 \times \text{CO}_2$ stabilization experiment with land-ice melting. *Clim Dyn* 29:521–534. doi:[10.1007/s00382-007-0250-0](https://doi.org/10.1007/s00382-007-0250-0)
- Swingedouw D, Mignot J, Braconnot P et al (2009) Impact of freshwater release in the North Atlantic under different climate conditions in an OAGCM. *J Clim* 22:6377–6403. doi:[10.1175/2009JCLI3028.1](https://doi.org/10.1175/2009JCLI3028.1)
- Tarasov L, Peltier WR (2003) Greenland glacial history, borehole constraints, and Eemian extent. *J Geophys Res Solid Earth* 108:n/a–n/a. doi:[10.1029/2001JB001731](https://doi.org/10.1029/2001JB001731)
- Valdes P (2011) Built for stability. *Nat Geosci* 4:414–416. doi:[10.1038/ngeo1200](https://doi.org/10.1038/ngeo1200)
- Van de Berg WJ, van den Broeke M, Ettema J et al (2011) Significant contribution of insolation to Eemian melting of the Greenland ice sheet. *Nat Geosci* 4:679–683. doi:[10.1038/ngeo1245](https://doi.org/10.1038/ngeo1245)
- Weaver AJ, Sedláček J, Eby M et al (2012) Stability of the Atlantic meridional overturning circulation: a model intercomparison. *Geophys Res Lett*. doi:[10.1029/2012GL053763](https://doi.org/10.1029/2012GL053763)
- Zeebe RE (2013) Time-dependent climate sensitivity and the legacy of anthropogenic greenhouse gas emissions. *Proc Natl Acad Sci*. doi:[10.1073/pnas.1222843110](https://doi.org/10.1073/pnas.1222843110)